ISSN 1512-0325

JOURNAL OF THE GEORGIAN CERAMISTS' ASSOCIATION

CERAMICS

AND ADVANCED TECHNOLOGIES

Scientific, technical and industrial illustrated, registered, referral magazine

Vol. 25. 1(49).2023

CONTENTS

UDC 666.1

INVESTIGATION OF BASALTS OF THE NORTH-TAFANI AREA OF THE BOLNISI DISTRICT IN ORDER TO OBTAIN GLASS AND GLASS-CRYSTALLINE MATERIALS

L. Gabunia, I. Kamushadze, E. Shapakidze, T. Petriashvili, M. Makadze

Ivane Javakhishvili Tbilisi State University. Caucasian Alexandre Tvalchrelidze Institute of Mineral Resources. 11, Mindeli str. 0186 Tbilisi. Georgia

E-mail: elena.shapakidze@tsu.ge

Resume: ***Goal.*** The work is devoted to the study of basalts of the Bolnisi district (North-Tafani area) with the aim of using them in the production of glass and glass-crystals as the main raw material component.

Method. For mineral-petrographic analysis, a polarizing microscope "МИМ" Р-113 was used.

The X-ray phase analysis were carried out using "ДРОН-1.5" diffractometer with A-Cu+C. U=35kv. I=20mA. Intensity - 2 degrees/min. λ=1.54178 Å.

Results. Comprehensive studies were carried out on two types of basalts of the North-Tafani. Under laboratory conditions, the chemical and mineral compositions of raw materials were determined; the ability to transition to a vitreous state; technological and physical-chemical properties of the melt, both separately and jointly in a ratio of 50/50.

The study of crystallization properties in the temperature range of 800-1250℃ on the surface of the glasses, the effect of iridescence was revealed - the formation of a clear transparent film, which is a prerequisite for obtaining facing tiles with high decorative properties.

Conclusion. The conducted studies have confirmed the possibility of using two types of basalt as a raw material for the production of facing black tiles and glass-crystalline materials (cast stone).

Key words: basalt, glass, glass-crystalline material, cast stone, crystallization, facing tiles, perturgy.

1. INTRODUCTION

Numerous experiments have established that local basalts are one of the important raw materials that are successfully used in glass production [1]. Basalts belong to low-melting rocks, which is due to the optimal ratio of different types of fusible oxides in them together, which excludes additional processing of raw materials in the production of glass. In such cases, the melting of the rock takes place without traditional silicate transformations and purification stages, resulting in a high-quality glass mass. All this, in turn, helps to simplify the technological process and, accordingly, reduces energy and material costs. In such cases, the melting of the rock takes place without traditional silicate alterations and purification stages, resulting in a high-quality glass mass. All this, in turn, helps to simplify the technological process and, accordingly, reduces energy and material costs.

Based on long-term research, the effectiveness of basalts in the production of glass-facing tiles, fibrous and glass-crystalline materials when used in the form of mono-charge has been established [2, 3]. Among them, Marneuli basalt deserves special attention, on the basis of which technologies for the production of black facing tiles and fibrous materials were developed and introduced into production conditions [4-7].

Therefore, the study of basalts from other deposits was of some interest, especially since South Georgia is quite rich in basalts that have been less studied in this direction [3].

Therefore, the study of basalts from other deposits was of some interest, especially since South Georgia is quite rich in basalts that have been less studied in this direction.

The presented investigation involves the study of basalt located in the North-Tafani area of the Bolnisi district to determine the possibility of using it as the main raw material in the production of vitreous and crystalline materials.

2. MAIN PART

The North-Tafani basalt deposit is located in the Bolnisi district, on the Tafani plateau. Considering the mining-geological and technical-economic conditions, it is recommended for industrial use [8]. The volume of basalt reserves in category A+B+C-1 is 2889490 m^3.

There are two types of basalts at the deposit: Tafani-1 is a dark gray, fine-crystalline massive rock belonging to the group of olivine basalts (dolerites); And, Tafani-2 is grayish-reddish, fine-crystalline, with calcite inclusions, and also representative of olivine basalts (dolerites). At the deposit, both types are not separated from each other and differ in color.

The mineralogical composition of both types of basalts is practically identical. It consists of plagioclase 58-61%, olivine 14-18%, clinopyroxene 16-20%, and magnetite minerals 5-5.5%.

By chemical composition (Table. 1) both types of Tafani basalt differ little from each other in the content of oxides, belong to the group of basic rocks, where the content of SiO_2 is within 48.5%. It mainly contains oxides of Al, Fe, Ca, Mg, Na, K and a small amount of MnO_2, TiO_2, and P_2O.

To determine the possibility of using basalt in the form of mono-charge in the production of glass, first of all, its melting and homogenization temperatures were determined (Table 2). Melting of both types of basalt, finely divided into fractions of 3-5 mm, took place in a laboratory electric furnace, with a carborundum heater, in corundum crucibles.

The experiment revealed similar properties for both types of Tafani basalt: the heat treatment of both are characterized by a relatively low-temperature homogenization interval of 1420-1440°C. Exposure for 30 minutes at maximum temperature results in a homogeneous glassy mass of black color with good flowability without any inclusions.

It should be noted that this parameter is 40 °C lower compared to similar data of Marneuli basalt introduced into production.

When studying the crystallization properties of the obtained glasses in the temperature range of 800-1250 °C, the tendency of the glasses to crystallize was revealed. During heat treatment at 800°C, an iridescence effect was observed on the

surface of the Tafani-2 sample - the formation of a metallic silver color, which changes its color when the temperature rises to 900°, turning into a golden color with a purple hue. During the aging process at a temperature of 1000-1100°C, the number of crystalline formations increases, which are formed in the form of a crystal structure in the Tafani-1 sample.

Within the temperature range of 1100-1200°C, the ability of crystallization decreases, and the thickness of the crust decreases, therefore the vitreous phase prevails, which is completely free of crystal inclusions at the temperature of 1250-1260°C.

According to the chemical stability, the samples are characterized by a high indicator of alkali resistance, and the loss in the acid area rises to 15%, as is characteristic of basalts from other locations.

The firing temperature of glass products has been experimentally determined, which provides removal of internal stresses in glass products and gives stability to the structure obtained from the melt, protecting it from deformation (Fig. 2), so the interval tg - tf is 30°C wider than the firing temperature.

The determination of process parameters for basalt heat treatment reveals a significantly lower viscosity of the glasses in the high-temperature interval (1380-1440°C), which in turn affects the fluidity of the molten mass. The latter determines the glass melt flowability during production: the glass melt flowability at high fluidity is greater, and during casting the glass melt fills the metal mold completely without pressure and retains a mirror-like surface.

This phenomenon is especially important in the mechanized production of basalt glass facing tiles by the free casting method, since the external shape, dimensions, and thickness of glass tiles are determined by the low viscosity of the melt [4].

Laboratory experiments carried out in this direction gave us positive results. Due to the high fluidity, we were able to increase the size of the tile and reduce the thickness to 4-6 mm, which was almost impossible when using Marneuli basalt [5]. The performance properties of glass tiles are presented (Table 2).

As the study of crystallization properties of basalt has shown, during heat treatment in a certain temperature interval, glass acquires an equally developed crystalline structure in the whole volume, which is an important precondition for obtaining a material crystallizing in volume-cast stone.

According to the literature data [9-12], natural alkaline rocks with a SiO_2 content of less than 52% are recommended for petrurgic purposes, while an increased number of divalent oxides is desirable.

In addition to the chemical composition, the parameters of cast stone are determined by the structure of the material, the type of crystalline phases formed, and the size of the crystals, as well as the ratio of the crystallized and residual vitreous phase.

Table 1

Chemical compositions of raw materials and optimal samples

No	Samples	Oxide content, mas. %													
		Mois-ture,%	LOI	SiO_2	TiO_2	Al_2O_3	Fe_20_3 +FeO	CaO	MgO	MnO	Na_2O	K_2O	P_2O_5	SO_3	Cr_2O_3
1	Tafani-1	0,16	0,56	48,01	1,19	17,89	10,89	9,07	7,24	0,62	3,25	0,76	0,63	0,12	–
2	Tafani-2	0,17	0,43	48,61	1,20	16,97	10,46	9,57	7,02	0,67	3,36	0,92	0,68	0,02	–
3	Quartz sand	–	–	98,5	–	1,1	0,3	–	–	–	0,06	0,04	–	–	–
4	Dolomite	43,0	0,04	1,77	–	1,5	0,69	40,0	13,5	–	0,1	0,2	–	0,4	–
5	75T+9Q+ 15D+ +1Cr_2O_3*	–	–	46,98	0,93	14,68	7,79	15,3	8,69	0,5	2,28	0,54	1,14	0,12	1,08

**symbols: T – Tafani, Q – quartz sand, D dolomite,*

Table 2

Parameters of experimental glasses

No	Index of glasses	Glass-melting temperature, □	Homogenization temperature,℃	glass crystallization interval, ℃	Expansion ratio	glass annealing temperature□	t_g	t_f	Weight loss in solution		
									1N HCL	1N NaOH	H_2O
1	Tafani-1	1090-1140	1420-1440	800-1240	74,6	620	655	725	15,3	0,2	0,03
2	Tafani -2	1025-1130	1420-1440	800-1250	79,8	630	668	720	15,1	0,16	0,04
3	Tafani 1-2	1090-1140	1420-1440	800-1250	–	–	–	–	15,3	0,16	0,03

Table 3

Operational properties of glass tiles

Index of glasses	Heat resistance at ±50□, cycles	Frost resistance, freeze-thaw cycles	Weight loss by abrasion, g/cm^3	Water absorption, %
Tafani 1-2	More than 10	More than 50	0,73	0,001

Table 4

Optimal properties of cast stone samples

Sample composition	Weight loss by abrasion, g/cm^2	Weight loss in medium, %		
		1N HCL	1N NaOH	H_2O
75T + 9Q + 15D + 1Cr_2O_3	0,09	0,39	1,19	0,1

A necessary condition for obtaining a high-quality glass-crystal material is the monomi-nerality of its structure, which is characterized by a great ability to isomorphically replace the constituent oxides around the core. Pyroxene is considered to be a mineral that gives the crystallized material high physical and mechanical properties, and a catalyst is used to intensify the crystallization process.

The studied basalts with the specified SiO_2 and RO (table 1) content and the corresponding crystallization ability can be used as a promising raw material for the production of cast stone. Therefore, further experiments were carried out on the processing of the composition and acceptance technology of the cast stone.

In order to increase the crystallization activity of glasses and homogeneity of structure, the composition of basalt charge was adjusted to increase RO, and the addition of Cr_2O_3 as a catalyst for crystallization.

When the initial composition of basalt was changed with the addition of dolomite, the material's crystallization ability and crystal sizes increased, but a residual excess of the vitreous phase was observed, which was caused by a decrease in the amount of SiO_2 in the charge. To correct this shortcoming, the addition of quartz sand was used to replenish the optimal amount of SiO_2. As a result of the tests, optimal compositions were obtained, which are characterized by a uniformly crystallized medium-grained monolithic texture, an insignificant amount of residual glassy phase, and high mechanical properties (Table 4).

Experiments have established a technological regime for obtaining stone casting in laboratory conditions, which provides for cooking the charge in a laboratory electric furnace in corundum crucibles at a maximum temperature of 1450°C with an exposure of 1 hour. Then the furnace temperature is rapidly reduced to 1300-1350°C and kept at this temperature for 40-60 minutes. the hot mass is transferred to the crystallization temperature of 870-900°C with an exposure of 30 minutes. At the last stage, the furnace is turned off and the sample is cooled naturally.

Cast stone samples obtained under laboratory conditions are characterized by high wear resistance, and with high corrosion resistance in aggressive conditions (Table 4).

The study of the structure of stones by X-ray phase analysis revealed the monominerality of their structure. Pyroxene minerals are found here mainly in the form of augite and diopside. These minerals determine the mechanical strength and chemical resistance of the material in relation to aggressive media (Fig. 1)

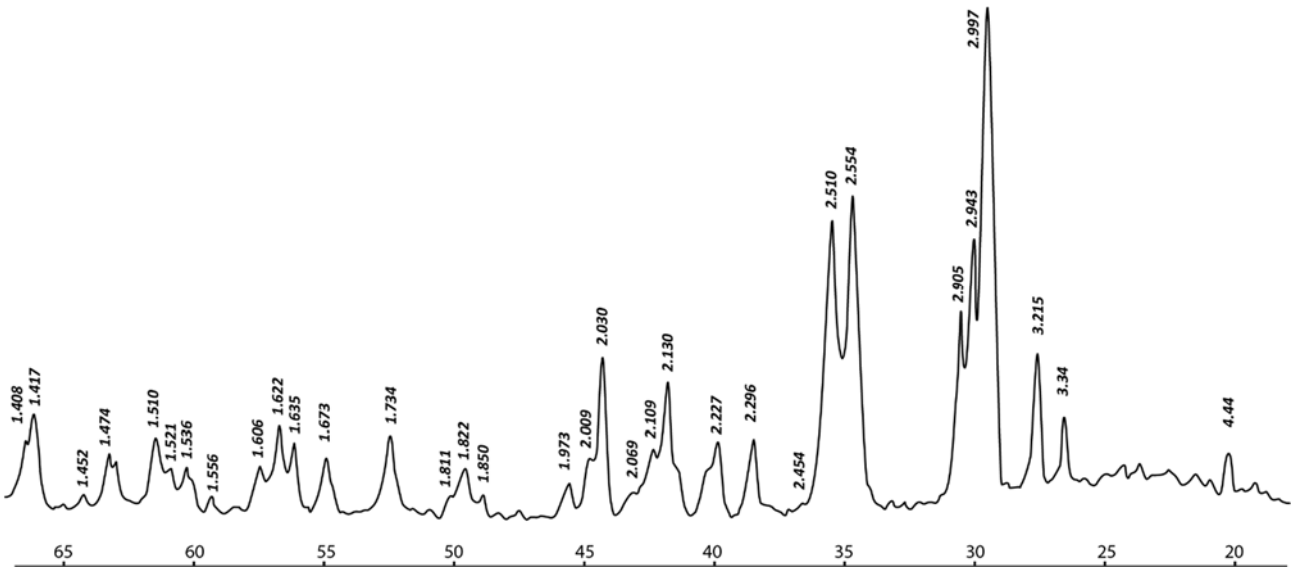

Fig. 1. X-ray phase analysis of optimal composition of cast stone

3. CONCLUSION

Thus, the conducted studies have confirmed the possibility of using two types of basalt from the Tafani area of the Bolnisi district as the main raw material in the production of facing black tiles and glass-crystalline materials (cast stone).

To thoroughly solve the problem, a more detailed study of the deposit is required to determine the uniformity and stability of the raw materials. The development of production based on them will allow us to turn the waste of the stone processing quarry into an acceptable inexpensive raw material for vitreous materials.

REFERENCES

1. Fibrous materials from basalts of Ukraine (collection of articles). (in Russian). Ed. “Tekhnika”. Kiev. 1974. 75 pp.
2. L. Gabunia, I. Kamushadze, D. Gagunashvili, R. Verulashvili. Investigation of Georgian basalts to obtain fibrous materials. (in Georgian). Proceedings of the Georgian Technical University No. 4 (453). Tbilisi, 2005, pp. 52-54.
3. L. Gabunia, Ts. Nafetvaridze, M. Alibegashvili. Research of basalts of South Georgia in order to use them in the production of fiber materials (in Georgian). Journal “Building materials and products”. No.3, 1997, Tbilisi, p. 2-5
4. R.D. Verulashvili, D.S. Gagunashvili, L.S. Khartishvili, I.G. Kamushadze, Yu. S. Rukhadze. Organization and development of mechanized production of black marblite glass tiles at the Experimental plant "GruzNIIstrom" (in Russian). Proceedings of the "GruzNIIstrom". Tbilisi, 1984, p. 148-153
5. K.A. Kostanyan, R.D. Verulashvili, I.G. Kamushadze, Yu.S. Rukhadze. Electric welding of iron-containing high-alumina alkaline glasses based on magmatic rocks to obtain marblite

tiles. (in Russian). Proceedings of the "Gruz-NIIstrom". Tbilisi, 1984, p. 24-30.

6. K. A. Gozalishvili, R. D. Verulashvili, L. S. Khartishvili, I. G. Kamushadze. Facing glass tiles with a colored surface film based on natural raw materials. (In Russian). Proceedings of the "GruzNIIstrom". Tbilisi, 1986, p. 116-123.
7. Patent of Georgia. “Composition of Basalt Fiber”. P3382 B AP 2004, 3431. AB 2004.06.10.
8. L.V. Ketskhoveli et al. About detailed exploration of the North-Tafani basalt deposit in the Bolnisi district for 1988-89 with the calculation of reserves (in Russian). Report of the Department of Geology of the GSSR, Tbilisi, 1989, p. 112.
9. Khan B. Kh., Bikov L. N. et al. Solidification and crystallization of stone casting (in Russian). Publishing house "Nauka Dumka", Kyiv, 1969, p. 147.
10. L. Gabunia, N. Gabunia, N. Jahva. The study of natural rocks in order to use vitreous materials in production. 2nd Conference of the International Ceramic Association. Proceedings of the Georgian Technical University. Tbilisi. 2009.
11. I. E. Lipovsky, V. A. Fedorov. Stone casting. (in Russian). Ed. “Metallurgy”. Leningrad, 1965.
12. Stonecast pipes based on basalt and andesite. L. V. Gabunia. Information leaflet on scientific and technological achievement. (in Russian). GruzNIINTI. 1983, Tbilisi.

UDC 541.49

QUANTUM-CHEMICAL STUDY OF AZELAIC ACID DIHYDRAZIDE MOLECULE USING THE AM1 METHOD IN DIFFERENT SOLVENTS

Z. Gogberashvili [1], M. Tsintsadze [1,2], N. Kilasonia [1,2], N. Gegeshidze [1,2], D. Lochoshvili [2]

[1] Georgian Technical University

[2] TSU R. Agladze Institute of Inorganic Chemistry and Electrochemistry

E-mail: m.tsintsadze@gtu.ge

Resume: **Goal:** The aim of the study is to investigate Azelaic Acid Dihydrazide as a promising organic ligand by Quantum Chemical Semi-Empirical AM1 method. Because Hdrazides are promising nitrogen-containing ligands, their study is of great importance for the synthesis of new coordination compounds, that have predetermined specific, unique properties and wide practical applications.The results of the research with this method allow to determine the dentate of the molecule, identify the donor atoms in it and their possibilities to participate in complex formation. Calculations are performed both for gas and for various solvents (Water, Ethanol, Methanol, Dimethylsulfoxide, Hexane, Acetone, Chloroform).

Method: quantum-chemical semi-empirical AM1 method.

Result: The obtained results allow us to conclude that the dihydrazide of azelaic acid can be presented as both a bidentate and a tetradentate ligand. From this point of view, this molecule is interesting for obtaining both homolithonic and heterolithonic complex compounds.

Conclusion. As the calculation results show, theoretically, the best environment for conducting the synthesis is dimethylsulfoxide as well as ethanol. This allows for the correct selection of the solvent in which the synthesis will be carried out for the next stage of the work, however, in addition to the theoretical data, the yield of the reaction should also be taken into account, and it is also possible that synthesis will be carried out using mixed solvents.

Key words: quantum-chemical; dentateness; Solvent organic ligand; complex formation; donor atom; complex forming; coordination compound.

1. INTRODUCTION

Our research considered the determination of the structure, structure and electronic characteristics of the polyfunctional ligand using a semi-empirical method, in particular the AM1 method. The object of research is azelaic acid dihydrazide.

2. MAIN PART

The potential energy distribution is calculated according to the density functional theory; Effective charges on atoms, electron distribution on atomic orbitals, electron density distribution, etc. are calculated. The advantage of performing

calculations in different solvents is that the synthesis of a complex compound can be planned in advance for this or that solvent. As a result of the calculations, those donor atoms (oxygen of the carbonyl group, nitrogen atoms of the hydrazide group) that can make a coordination bond with the metal-complex generator have been identified. The study of azelaic acid dihydrazide molecule is particularly interesting because it contains two hydrazide residues, which, compared to monobasic acid hydrazides, increases its coordination capabilities [1-3].

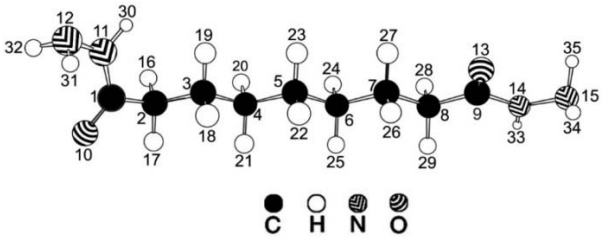

Numbering of atoms in azelaic acid dihydrazide molecule

Structural, energetic and electronic characteristics of azelaic acid dihydrazide molecule were calculated both for the gaseous state and in different solvents, which, in turn, are characterized by different dielectric permeability. Water, ethanol, methanol, dimethylsulfoxide, acetone, chloroform and hexane are selected as solvents. The heat of formation (kJ/mole) is negative in both gases and all solvents. Its lowest value is found in hexane [3, 5].

As for dipole moments, we have almost the same data in water, dimethylsulfoxide, ethanol and methanol. This circumstance is explained by the generation of an additional induced moment.

The calculation results show that interatomic distances, as well as valence angles, are slightly different, and the latter, in turn, indicate the influence of solvents on the parameters of azelaic acid dihydrazide molecule [1,2,4-6].

According to the data, the angles C(8)-C(9)-O(13); C(2)-C(1)-O(10); C(1)-N(11)-N(12); C(2)-C(1)-O(10) is mostly within 120-122°, which indicates the sp2 hybridized state of C(8) and C(9) atoms. The values of these angles are almost the same in all solvents, with a slight difference.

Bond lengths are also calculated for the azelaic acid dihydrazide molecule. As the bond length analysis shows, C – C and C – N interatomic distances in all solvents are within 1.398-1.400 and 1.382-1.192 Å. The length of the C – O bond is the same in both cases and varies slightly in the range of 1.250-1.252 Å for all solvents (Tab.1).

Electron occupancy of atomic orbitals and distribution of electron density on atoms show that on such atoms as e.g. The oxygen atoms of both carbonyl groups, O(7) and O(3), for any solvent considered, have high electronic density everywhere, ranging from about 6500 to 6.515. However, it should be noted that it reaches the highest value in water, followed by dimethylsulfoxide and ethanol.According to the calculation data (Tab 2.), the electron pair for the mentioned atoms is located on sp hybrid orbitals and has a pronounced s-nature. Therefore, it is possible that the oxygen atoms of the carbonyl group, O(10) and O(13), act as donor atoms and connect to the metal-complex producer through a coordination bond.

Tab.1

bond angles in the azelaic acid dihydrazide molecule

N	Valentic angle	Solvent							
		Air	H_2O, Water	C_2H_6SO, DMSO	CH_3OH, Methanol	C_2H_5OH, Ethanol	$(CH_3)_2CO$, Acetone	$CHCl_3$, Cloro-form	C_6H_{12}, Hexane
1	C(1)–C(2)–C(3)	112.043	113.031	112.957	112.690	112.787	112.638	112.205	111.763
2	C(2)–C(3)–C(4)	110.727	110.392	110.418	110.505	110.366	110.573	110.483	110.674
8	C(2)–C(1)–O(10)	122.136	120.683	120.660	120.900	120.727	121.079	121.396	121.856
9	C(2)–C(1)–N(11)	117.460	119.224	119.226	118.913	119.140	118.641	118.351	117.769
10	C(1)–N(11)–N(12)	126.175	126.503	126.410	126.265	126.380	126.184	126.290	126.229
11	C(8)–C(9)–O(13)	123.299	121.910	121.764	122.036	122.036	122.345	122.932	123.129
12	C(8)–C(9)–N(14)	116.586	118.152	118.262	118.030	118.047	117.700	117.119	116.847
13	C(9)–N(14)–N(15)	126.231	125.998	125.798	125.804	126.223	125.993	126.264	126.217
14	C(1)–C(2)–H(16)	109.490	108.057	108.366	108.482	108.799	108.435	109.009	109.591
15	C(1)–C(2)–H(17)	107.268	107.692	107.560	107.352	107.555	107.560	107.475	107.234
16	C(2)–C(3)–H(18)	109.669	109.803	109.918	110.095	109.798	110.132	109.799	109.803
17	C(2)–C(3)–H(19)	110.221	110.555	110.363	109.995	110.479	109.837	110.321	110.045
27	C(7)–C(8)–H(29)	109.822	110.189	110.238	110.210	110.229	110.127	109.907	109.878
28	C(1)–N(11)–H(30)	120.148	119.912	119.749	119.786	119.663	119.176	119.876	120.004
29	N(11)–N(12)–H(31)	109.332	109.374	109.322	109.144	109.597	109.058	109.521	109.396
30	N(11)–N(12)–H(32)	108.756	109.502	109.452	109.666	109.172	109.763	109.130	108.904
31	C(9)–N(14)–H(33)	120.423	119.011	118.700	118.923	119.436	118.916	119.996	120.240
32	N(14)–N(15)–H(34)	109.097	110.097	110.096	110.088	109.724	109.951	109.241	109.120
33	N(14)–N(15)–H(35)	108.974	108.958	108.879	108.899	109.086	108.968	109.410	109.148

Tab.2.

charges on atoms (q), electron density and electron distribution on atomic orbitals (s,p) calculated by semiempirical quantum-chemical AM1 method

N	Solvent	Atom	Charge on an Atom	Electron density per atom	n	Allocation of electrons to orbitals			
						nS	nP_x	nP_y	nP_z
1	Air	C(1)	0.283	3.717	2	1.236	0.901	0.768	0.812
		C(9)	0.283	3.717	2	1.236	0.809	0.916	0.756
		O(10)	-0.372	6.372	2	1.917	1.673	1.439	1.343
		N(11)	-0.352	5.352	2	1.470	1.026	1.624	1.231
		N(12)	-0.173	5.173	2	1.634	0.912	1.200	1.427
		O(13)	-0.371	6.371	2	1.917	1.622	1.379	1.453
		N(14)	-0.357	5.357	2	1.469	1.079	1.084	1.726
		N(15)	-0.172	5.172	2	1.634	1.399	1.012	1.128
		H(30)	0.251	0.749	1	0.749			
		H(31)	0.140	0.860	1	0.860			
		H(32)	0.143	0.857	1	0.857			
		H(33)	0.251	0.749	1	0.749			
		H(34)	0.141	0.859	1	0.859			
		H(35)	0.141	0.859	1	0.859			
2	H_2O, Water	C(1)	0.340	3.660	2	1.237	0.907	0.743	0.772
		C(9)	0.340	3.660	2	1.239	0.792	0.893	0.735
		O(10)	-0.562	6.562	2	1.915	1.721	1.485	1.440
		N(11)	-0.314	5.314	2	1.467	1.027	1.485	1.335
		N(12)	-0.250	5.250	2	1.629	0.917	1.301	1.404
		O(13)	-0.547	6.547	2	1.915	1.679	1.499	1.454
		N(14)	-0.320	5.320	2	1.479	1.230	1.121	1.490
		N(15)	-0.255	5.255	2	1.628	1.280	0.998	1.349
		H(30)	0.294	0.706	1	0.706			
		H(31)	0.182	0.818	1	0.818			
		H(32)	0.181	0.819	1	0.819			
		H(33)	0.294	0.706	1	0.706			
		H(34)	0.176	0.824	1	0.824			
		H(35)	0.183	0.817	1	0.817			

3	C_2H_6SO, DMSO	C(1)	0.340	3.660	2	1.237	0.907	0.744	0.771
		C(9)	0.338	3.662	2	1.240	0.797	0.903	0.722
		O(10)	-0.559	6.559	2	1.915	1.721	1.481	1.442
		N(11)	-0.315	5.315	2	1.467	1.027	1.477	1.343
		N(12)	-0.249	5.249	2	1.629	0.917	1.303	1.400
		O(13)	-0.542	6.542	2	1.915	1.677	1.455	1.496
		N(14)	-0.319	5.319	2	1.483	1.218	1.104	1.514
		N(15)	-0.255	5.255	2	1.629	1.269	1.011	1.345
		H(30)	0.293	0.707	1	0.707			
		H(31)	0.181	0.818	1	0.818			
		H(32)	0.180	0.819	1	0.819			
		H(33)	0.292	0.708	1	0.708			
		H(34)	0.175	0.825	1	0.825			
		H(35)	0.183	0.817	1	0.817			
4	CH_3OH, Methanol	C(1)	0.339	3.661	2	1.238	0.908	0.739	0.777
		C(9)	0.338	3.662	2	1.239	0.812	0.915	0.695
		O(10)	-0.553	6.553	2	1.915	1.717	1.487	1.434
		N(11)	-0.315	5.315	2	1.469	1.027	1.497	1.322
		N(12)	-0.249	5.249	2	1.629	0.918	1.285	1.418
		O(13)	-0.538	6.538	2	1.915	1.682	1.349	1.592
		N(14)	-0.323	5.323	2	1.481	1.106	1.084	1.652
		N(15)	-0.253	5.253	2	1.628	1.351	1.071	1.203
		H(30)	0.292	0.708	1	0.708			
		H(31)	0.181	0.819	1	0.819			
		H(32)	0.179	0.821	1	0.821			
		H(33)	0.291	0.709	1	0.709			
		H(34)	0.175	0.825	1	0.825			
		H(35)	0.182	0.818	1	0.818			
5	C_2H_5OH,Ethanol	C(1)	0.337	3.663	2	1.237	0.907	0.747	0.772
		C(9)	0.339	3.661	2	1.238	0.797	0.901	0.725
		O(10)	-0.549	6.549	2	1.915	1.719	1.489	1.426
		N(11)	-0.317	5.317	2	1.468	1.026	1.498	1.325
		N(12)	-0.247	5.247	2	1.629	0.917	1.272	1.429
		H(20)	0.088	0.912	1	0.912			
		H(21)	0.087	0.913	1	0.913			
		H(22)	0.085	0.915	1	0.915			

		H(23)	0.084	0.916	1	0.916			
		H(24)	0.086	0.914	1	0.914			
		H(25)	0.086	0.914	1	0.914			
		H(26)	0.094	0.906	1	0.906			
		H(27)	0.091	0.909	1	0.909			
		H(28)	0.128	0.872	1	0.872			
		H(29)	0.140	0.860	1	0.860			
		O(13)	-0.539	6.539	2	1.915	1.666	1.466	1.492
		N(14)	-0.325	5.325	2	1.473	1.165	1.115	1.572
		N(15)	-0.249	5.249	2	1.629	1.341	1.009	1.270
		H(30)	0.291	0.709	1	0.709			
		H(31)	0.178	0.822	1	0.822			
		H(32)	0.180	0.820	1	0.820			
		H(33)	0.293	0.707	1	0.707			
		H(34)	0.175	0.824	1	0.824			
		H(35)	0.180	0.820	1	0.820			
6	$(CH_3)_2CO$,Acetone	C(1)	0.337	3.667	2	1.238	0.908	0.731	0.787
		C(9)	0.337	3.663	2	1.239	0.818	0.900	0.706
		O(10)	-0.544	6.544	2	1.915	1.714	1.490	1.424
		N(11)	-0.316	5.316	2	1.473	1.027	1.524	1.293
		N(12)	-0.248	5.248	2	1.629	0.919	1.259	1.441
		O(13)	-0.530	6.530	2	1.914	1.706	1.325	1.585
		N(14)	-0.327	5.327	2	1.480	1.041	1.133	1.673
		N(15)	-0.250	5.250	2	1.629	1.394	1.108	1.119
		H(30)	0.289	0.711	1	0.711			
		H(31)	0.181	0.819	1	0.819			
		H(32)	0.177	0.823	1	0.823			
		H(33)	0.289	0.711	1	0.711			
		H(34)	0.173	0.827	1	0.827			
		H(35)	0.181	0.819	1	0.819			
7	$CHCl_3$, Cloroform	C(1)	0.323	3.677	2	1.237	0.906	0.742	0.792
		C(9)	0.325	3.675	2	1.236	0.809	0.918	0.711
		O(10)	-0.493	6.493	2	1.916	1.702	1.493	1.383
		N(11)	-0.331	5.331	2	1.469	1.027	1.578	1.258
		N(12)	-0.229	5.229	2	1.630	0.917	1.230	1.454
		O(13)	-0.483	6.483	2	1.915	1.641	1.382	1.545

		N(14)	-0.343	5.343	2	1.470	1.049	1.074	1.749
		N(15)	-0.229	5.229	2	1.629	1.438	1.36	1.126
		H(30)	0.279	0.721	1	0.721			
		H(31)	0.168	0.832	1	0.832			
		H(32)	0.171	0.829	1	0.829			
		H(33)	0.280	0.720	1	0.720			
		H(34)	0.169	0.831	1	0.831			
		H(35)	0.167	0.833	1	0.833			
8	C_6H_{12},Hexane	C(1)	0.303	3.697	2	1.236	0.903	0.752	0.806
		C(9)	0.304	3.696	2	1.236	0.806	0.907	0.747
		O(10)	-0.428	6.428	2	1.916	1.686	1.471	1.355
		N(11)	-0.344	5.344	2	1.469	1.026	1.624	1.224
		N(12)	-0.202	5.202	2	1.632	0.915	1.196	1.460
		O(13)	-0.423	6.423	2	1.916	1.645	1.402	1.461
		N(14)	-0.352	5.352	2	1.469	1.081	1.116	1.687
		N(15)	-0.201	5.201	2	1.632	1.401	1.020	1.149
		H(30)	0.264	0.736	1	0.736			
		H(31)	0.154	0.846	1	0.846			
		H(32)	0.158	0.842	1	0.842			
		H(33)	0.265	0.735	1	0.735			
		H(34)	0.155	0.845	1	0.845			
		H(35)	0.155	0.845	1	0.845			

When comparing the electron density and atomic orbitals, the difference between these parameters for these atoms is not significantly different, however, comparing the nitrogen atom of the NH_2 group with the electron band of N(11) and N(12), N(14) and N(15) of the nitrogen atoms of the hydrazide group. with the atom shows that the electronic excitability of the latter is slightly less in all solvents. Nevertheless, it is likely that the formation of a coordination bond with the metal-complexing agent is more possible with the nitrogen atom of NH_2, because, if we take into account the ability of oxygen atoms to coordinate, in such a case it is possible to form five-membered metallocycles, where azelaic acid dihydrazide is coordinated in a keto or enol form [7-13].

We can judge the possibility of the existence of enolic form both by literary data and by the results of calculations - according to the lack of electrons and high positive charge on H(30) and H(33) hydrogen atoms.

3. CONCLUSION

If we summarize the results of the calculations, we can conclude that the dihydrazide of azelaic acid can be presented as both bidentate and tetradentate

ligand. From this point of view, this molecule is interesting for obtaining both homolithonic and heterolithonic and mixed ligand complex compounds [14-16].

REFERENCES

1. M. Tsintsadze, N. Frangishvili, N. Kilasonia, M. Mamiseishvili, G. Tsintsadze - research of the electronic structure of the isonicotinoylhydrazone molecule of acetone and the complex formation ability in different solvents. Proceedings of Technical University of Georgia. "Technical University", 2019. p. 73-81.
2. M. Tsintsadze, N. Kilasonia, Z. Gogberashvili, N. Gegeshidze. Synthesis and physico-chemical properties research of mixed ligand coordination compounds with para-dimethylaminbenz aldehyde nicotinoylhydrazone and 2-amino-6-methylpyridine. VIII Inter.Scien.Conf. "The Chemistry of coord. compounds" dedicated to the 85th anniversary of the Department of Analytical Chemistry. Baku 2020.
3. V. Skopenko, G. Tsintsadze, L. Savranski, M. Tsintsadze. Coordination chemistry. Editorial-Publishing Council of the National Academy of Sciences of Georgia, Tbilisi, 2012. 450 p.
4. T. Tsintsadze, N. Tabuashvili, M. Tsintsadze, D. Lochoshvili, N. Kilasonia, N. Gegeshidze. Quantum-chemical study of electronic structure and complex formation ability of isonicotinoyl-hydrazone of paradimethylaminobenzaldehyde. Science of Georgia Bulletin of the Academy, Chemistry Series, Vol. 37, N1-2. pp. 104-110. 2011.
5. Reichard Ch., Welton Th. Solvents and solvent EEfects in organic chemistry. 2010. https://onlinelibrary.wiley.com/doi/book/10.1002/9783527632220
6. Tsintsadze G.V., Kereselidze J.A., Tsintsadze M.G., Kurtanidze R.Sh., Giorgadze T.Z., Taktakishvili T.T. // Quantum-chemical study of the benzoylhydrazonebenzaldehyde molecule. Georgian Enginering News. 2000. №4. C. 115-117.
7. M. Tsintsadze, T. Tsintsadze, N. Kilasonia, D. Lochoshvili, N. Tabuashvili, N. Gegeshidze. The way of coordination of ortho-aminopyridine-metilderivatives with metals (influence of solvent on the ability of complexcreation). 2-nd International conferenceon Organic Chemistry -"Advances inHeterocyclic Chemistry". 2011. P.103.
8. Miminoshvili È. B., X-Ray Diffraction Study of Coordination Compounds of Biometals(II) with Carbonic Acid Hydrazides, Guanidine and Aminoguanidine Obtained by Chemical Synthesis, Diss. … Doct. Chem. Sciences, State Technical University, Tbilisi 2003.
9. Tsintsadze M.G. Coordination compounds of metals with nitrogen- and oxygen-containing ligands - derivatives of the aliphatic, aromatic and heterocyclic series. National Academy of Sciences of Georgia. Tbilisi 2008. 247 p.
10. Tsintsadze G.V., Kereselidze J.A., Tsintsadze M.G., Kurtanidze R.Sh., Giorgadze T.Z., Taktakishvili T.T. Quantum-chemical study of the benzoyl hydrazonebenzaldehyde molecule. Georgian Engineering News. 2000. No. 4. C. 115-117.
11. Tsintsadze M., Mamiseishvili M., Kilasonia N., Lochoshvili D., Gegeshidze N., Giorgadze T. Study of the electronic structure of para-dimethylaminobenzaldehyde para-nitrobenzoyl

hydrazone and complex forming ability by quantum-chemical semiempirical AM1 method. Chemical Journal of Georgia, Vol. 9, 2009. N4. pp. 301-302.

12. M. Tsintsadze, N. Kilasonia, N. Tabuashvili, N. Gegeshidze. Synthesis and IR absorption speqtra of mixed-ligand coordination compounds of copper(II), manganese(II), cobalt(II) and nickel(II) with ortho-amino-4-methylpyrydine and paradimethyl aminobenzaldehyde isonicotinoilhidrazone. 3-rd International Conference of young Scientists. 2013. Abstyracts. p.103.
13. M. Tsintsadze, N. Gegeshidze, N. Kilasonia, D. Lochoshvil i, S. Gelovani - Study of the effect of solvents on the complexing ability of picolinamide molecules by semi-empirical quantum chemical method AM1. Kyiv Conference on Analyticai Chemistry Modern Trends. Book off Abstracts. Київ. 2022. p.54-55.
14. T. Giorgadze, I. Sharia, M. Tsintsadze, D. Lochoshvili, G. Tsintsadze. Influence of the solvent on the complexing ability of meta-nitrobenzoyl hydrazone of meta-nitrobenzaldehyde (MNBGMNBA). Int. Scientific-tech. conf. "Nature protection and sustainable development" dedicated. 80 years old. Prof. V.Eristavi. Collection of works. Tbilisi. 2020. pp.164-166.
15. M. Tsintsadze, T. Giorgadze, I. Sharia. Defining the complex formation ability of a hydrazone (para - nitrobenzoylhydrazoneof meta-nitrobrobenzaldehyde (PNBHMNBA) Containing carbonyl group. Online Conference. “Chemical and Technologicai aspects of Biopolimers” Book. Volume I. Tbilisi 2020. p.157-167.
16. Z. Gogberashvili, M. Tsintsadze, N. Kilasonia, G. Tsintsadze. Research, coordination mixed ligands compounds of cobalt with usethermogravimetric and absorption by infrared spectroscopy methods. Inter.Scientific conf. “Environmental protection and sustainable devopment” dedicated to Prof. Victor Eristavi. Book of Abstracts. Tbilisi 2019. p. 26.

UDC 666.76

HIGH REFRACTORY COMPOSITES ON THE BASIS OF SILICON CARBIDE

Z. Kovziridze. N. Nizharadze, V. Qinqladze, N. Darakhvelidze, M. Balakhashvili, Ts. Danelia

Institute of Bionanoceramic and Nanocomposite Technology. Georgian Technical University, Tbilisi, 0175, Kostava str. 69

E-mail: kowsiri@gtu.ge

Resume: **Goal.** High refractory composite on the basis of silicon carbide base with complex binder is received with burning of SiC-Si and clay mixture in nitrogen medium at temperature 1420^{0}C. The composition of silicon carbide binder is stated the main component of which is silicon oxynitride – Si_2ON_3.

Method. Microstructure and phase composition of the received composites are studied with X-ray structural, raster electron-microscopic and optical analysis.

Results. From the mentioned composite material (SiC-l) and with addition of 30% aluminum oxide nano-powder (SiC-2) the samples are hot pressure moulded in vacuum at 1600^{0}C, with pressure 16 MPa and with 5-7 minutes delay at the last temperature.

Some physical-mechanical properties of samples received with initial and hot pressure are investigated. The mechanical factors of the samples obtained with hot pressure are: ultimate compression strength - 1465 MPa, HRA – 92, for samples obtained with addition of Al_2O_3 are 1598 MPa, HRA – 93, respectively.

Conclusions. The high exploitation indices of the obtained composites determine the use of silicon carbide products in structural materials.

Key words: silicon carbide; microstructure; X-ray structural analysis; hot pressure.

1. INTRODUCTION

Silicon carbide and materials on its basis are distinguished with high mechanical indices at high temperature, resistance to aggressive media, wear resistance, etc. Therefore, researches are in progress, as the possibilities of material science in silicon carbide sphere are not yet exhausted [1-4].

For realization of potential possibilities of this compound the creation of high density materials and items technology is necessary, which ensures their use in constructive purposes. The particular problems arise at realization of sintering process which is hampered because of strong covalent bonds and low mobility of atoms in silicon carbide crystalline lattice.

In sintering process material transportation is particularly activated when using such method of solidification when material is simultaneously affected with high temperature and pressure, i.e. when using hot pressure method. Simultaneous influence of temperature and pressure accelerates the process of material transportation in liquid and solid phases contact zone [5-6].

The regulation of liquid phase amount, of the temperature of its origination in case of silicon

carbide sintering is achieved with introduction of special additives, of oxide additives, as a rule.

These sintering activating additives participate in phase shaping and microstructure formation. In such a way they help and have important effect on service properties of the sintered material.

2. MAIN PART

Using silicon carbide matrix the composite is received with reactive sintering method when burning silicon carbide, silicon and refractory clay mixture in (technical) nitrogen medium unpurified from oxygen [7-10] at 1420^{0}C temperature.

We studied phase composition, microstructure and some physical-technical properties of the mentioned composite and samples received with hot pressure method of the same composite. The results are presented in this work.

From the mixture of silicon carbide, silicon and Chasov-Yar ore refractory clay, the material composition of which is presented in Table 1, we prepared sample-cylinders with sizes d-15 mm, h-15mm, moulded them under 200 MPa pressure with semi-dry method. After drying, the samples were burned in furnace at temperature 1420^{0}C in nitrogen medium with 2 hours delay at the last temperature. The rate of temperature rise was 250^{0}C/h. The properties of the received samples were studied and the physical-mechanical indices are given in Table 1.

The received samples were broken, grounded and two powders were prepared for receiving samples with hot pressure method (Table 2). As is seen from the Table, SIC-1 is powder sample received with reactive sintering method, SIC-2 is material received with addition to the previous sample of 30% Al_2O_3 nano-powder. As was mentioned above, the receiving of solid material on the basis of silicon carbide powder requires the selection and introduction of such additives which support sintering process as a result of liquid phase creation.

In our composition in order to receive samples with hot pressure method and for improvement of material sintering process, magnesium oxide and rare earth element - yttrium oxide Y_2O_3 - were used as additives. High melting temperature of these oxides ensures formation of high temperature eutectic melt in mixture, which will promote the process of material sintering. This has an essential importance for receiving items of high thermal resistance and strength.

MgO and Y_2O_3 were added to powder above 100% in amounts 1 and 1.5%, respectively.

Hot pressure temperature was 1600^{0}C. Pressurization pressure was 16 MPa. Delay of 5-7 minutes at the last temperature. Heating was performed in vacuum. For investigation of samples received with reactive sintering and hot pressure method the comparative tests had been carried out for all compositions, for determination of the following property indices: compressive strength, open porosity, thermal resistance, density and hardness.

If we compare property values which are chosen as indices and are given in Tables 1 and 2, we can notice moulding method effect on physical-mechanical indices.

Compressive strength and open porosity (Tabl. 2) of samples received with hot pressure changed abruptly for SIC-1 samples compared to the

respective indices of SK samples received with reactive sintering method. Introduction of Al_2O_3 nano-powder into SiC-1 composition also improves all indices.

Ultimate compression strength for SiC-1 is equal to 1465 MPa while for SK samples received with reactive sintering the same index is 120 MPa. Open porosity in the first case is 2.9%, in the second one – 16.8 %. The introduction of Al2O3 nano-powder into SiC-1 composition improves all indices. Ultimate compression strength is 1599.8 MPa, open porosity - 1.2%, hardness - 93 HRA, thermal resistance is > 50 thermal exchange [11-14].

Compared to SiC values phase composition of samples before and after pressurization was determined with X-ray structural analysis with of diffractometer DPOH-3. Structural research was done by means of microscope.

Table 1

Material composition of charge and properties of the received samples

Index	Components, mass.%				Physical-mechanical indices				
	SiC	Si	Clay	Pressure of moulding, MPa	Open porosity, w%	Density, g/cm^3	Ultimate compression strength, MPa	Thermal stability, Heat exchange	Refractoriness, ^oC
SK	75	13.5	11.5	20	16.8	2.88	120	25	1770

Table 2

Properties of samples received with hot pressure

Index	Components, mass%				Burning tempe-rature, T^0C	Mouldin g pressure, MPa	Delay at last tempera - ture min.	Physical-mechanical properties				
	SK	Al_2O_3	MgO	Y_2O_3				Open porosity, %	Ultimate compres-sion strength, MPa	Hardness, HRA	Density, g/cm^3	Thermal resis-tance, Heat exchange
SiC-1	100	-	1	1.5	1600	16	5-7	2.9	1465.0	92	3.08	40
SiC-2	70	30	1	1.5	1600	16	5-7	1.2	1599.8	93	3.19	50

According to microscopic analysis the basic part of SIC-1 consists of distinctly differing coarse and medium size silicon carbide grains. The interval between grains is filled with binder (Fig.1 a, b) which represents glassy phase received as a result of clay burning, which contains quite great amount of silicon oxynitride (Si_2ON_2). It represents the main component of binder. Small amount of mullite crystals are noticed, which are also formed at clay heating at high temperature. This figure is more clear at microscopy magnification, particularly: at X200 and 500 magnification (Fig.1 c,d). The Figures show that silicon carbide grains are isolated from each other and intervals between them are filled with well sintered binder.

Compared to SiC-1, structure of SiC-2 is different (Fig.2). The main component here is again silicon carbide, but it is not coarse grain. Grains are medium and fine crystalline. In this sample there are well crystallized corundum grains, which are quite fine crystalline. It differs from SiC-1 in that in this sample there is a great amount of mullite crystals, which are generated as a result of internal molecular transformations of clay and with interaction of Al_2O_3 added, to charge with clay component SiO_2.

The distinct difference between these two samples is also that SiC-1 structure (Fig.1) is inhomogeneous while SiC-2 (Fig.2) is homogeneous, the binding mass of which contains compactly packed crystals. None of the samples contains pores. The X-ray structural analysis of these samples coincides with microscopic research data.

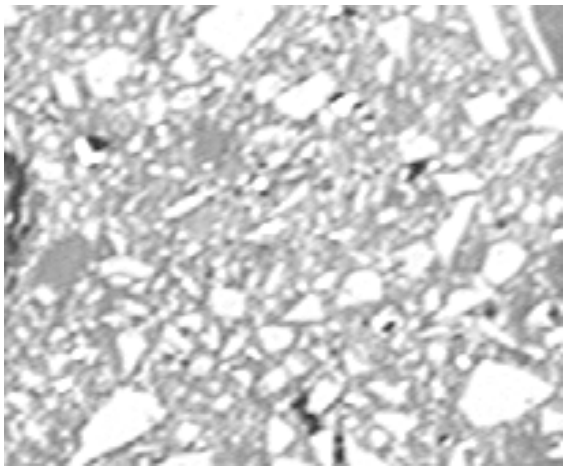

a)

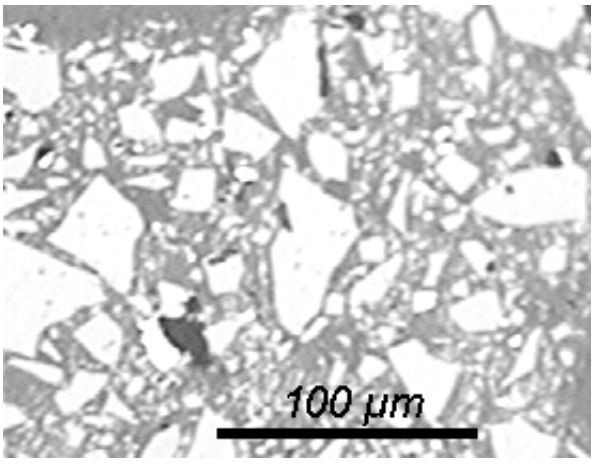

b)

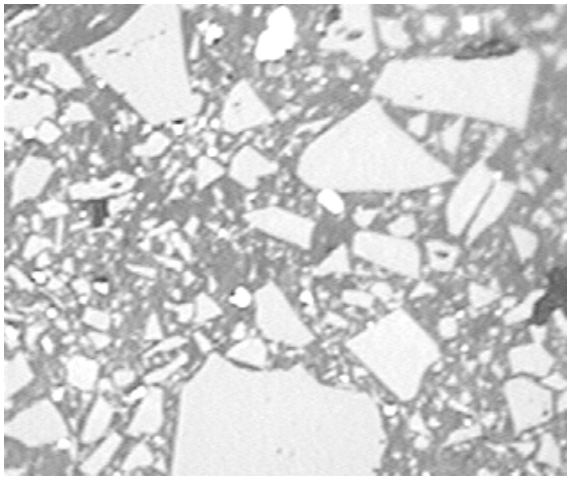

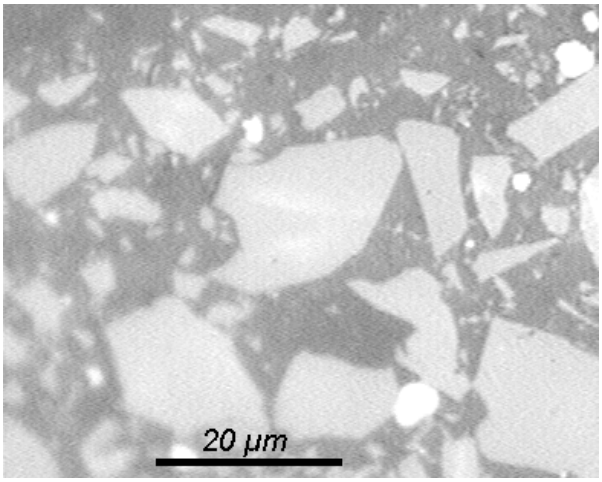

c) d)

Fig.1. SiC-1 refractory microstructure at different expansion:
a) x50 b) x100; c) x200; d) x500.

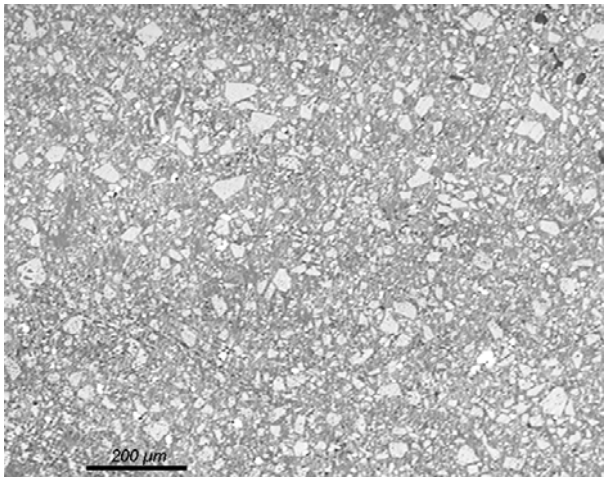

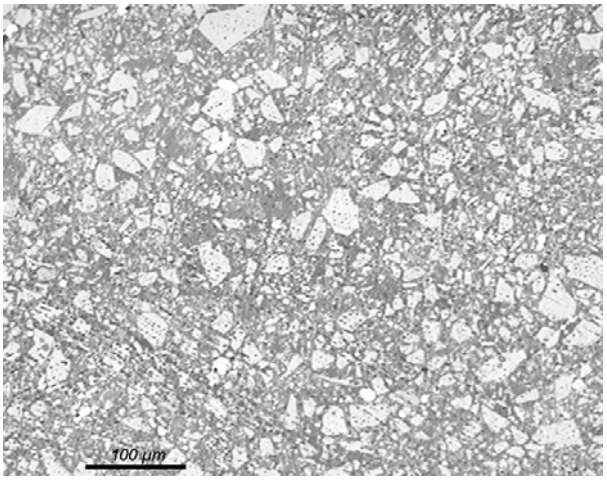

a) b)

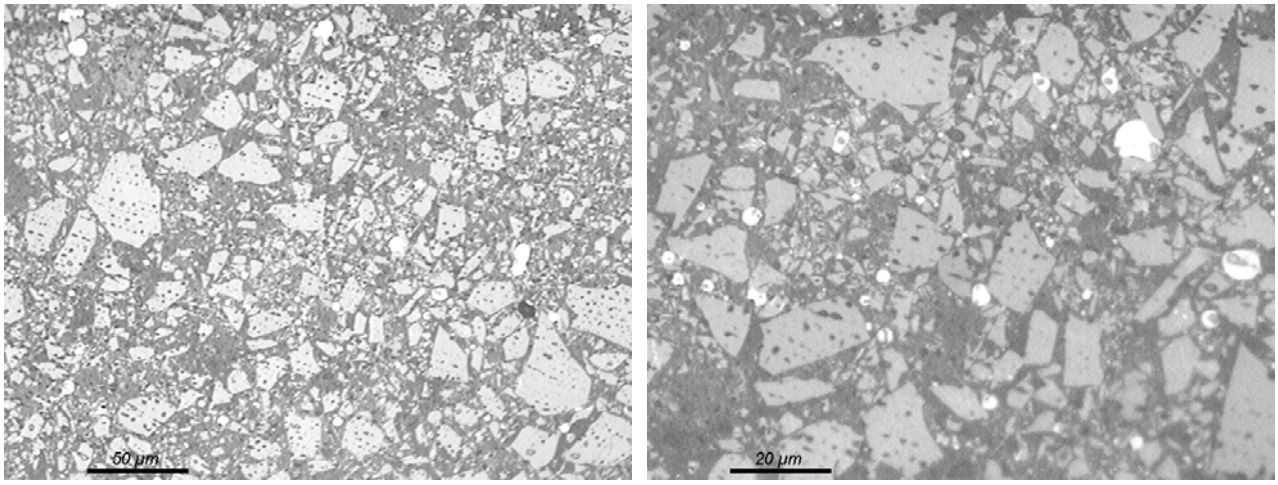

c) d)

Fig.2. SiC-2 refractory microstructure at different expansions:
a) x50; b) x100; c) x200; d) x500.

In X-ray of the initial sample (Fig.3) the following phases are fixed: silicon carbide – SiC - d_{hkl} 2.627; 2,52; 2,39; 2,36; 2.176; 2.000Å; silicon oxinitride Si_2ON_2 - d_{hkl} 4.70; 4.47; 3.38; 2.745; 2.43; 2.395; 1.088; 1.79; 1.774Å; silicon Si - d_{hkl} 3.145; 1.919Å; SiO_2 - d_{hkl} 4.06Å silicon nitride, Si_3N_4 - d_{hkl} 2.745; 2.581Å.

In X-ray of SiC-1 sample, received with hot pressure, there is silicon carbide peak of the same intensity and silicon oxynitride lines of the same intensity as in the initial sample. There is no silicon here and silicon nitride was fixed in small intensity – Si_3N_4 - d_{hkl} 2.575Å. Mullite was detected neither in the initial sample nor in the samples received with hot pressure.

In X-ray of Al_2O_3 containing SiC-2 the silicon carbide peaks are of the same intensity, Al_2O_3 - d_{hkl} 3.476; 2.385; 2.08; 1.600Å, so are diffraction maximums characterized to Si_2ON_2 - d_{hkl} 4.64; 4.44; 3.38; 2.80Å, silicon nitride d_{hkl} 2.666; 1.740Å. Silicon is not present here either. Different from SiC-1 samples here is mullite d_{hkl} 5.37; 3.616; 3.38Å. The comparatively low intensity peaks of Al_2O_3 is explained with the fact that here its part is spent for creation of mullite [15-19].

Fig.3 presents X-ray of the initial sample and in Fig 4 – X-ray of SiC-1 and SiC

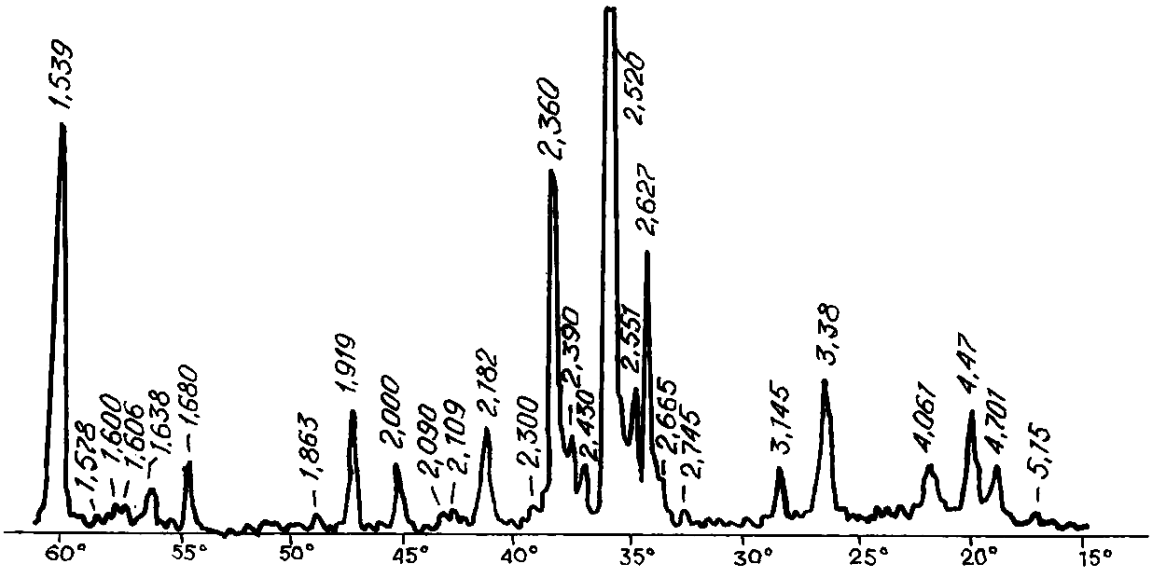

Fig. 3. X-ray of the initial sample

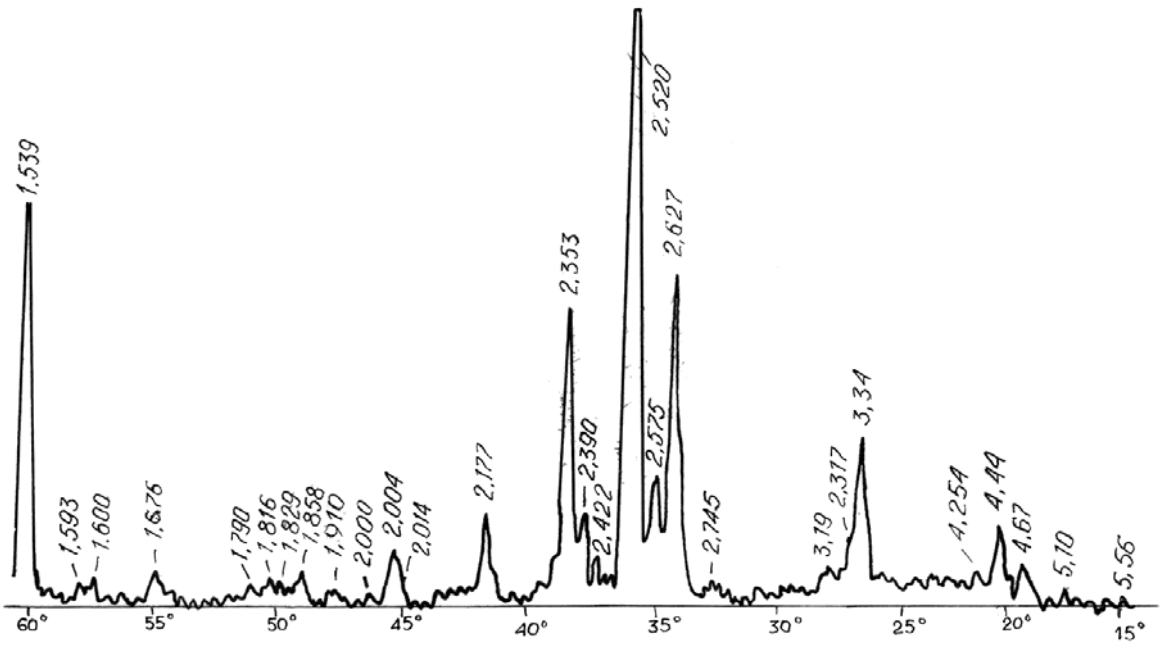

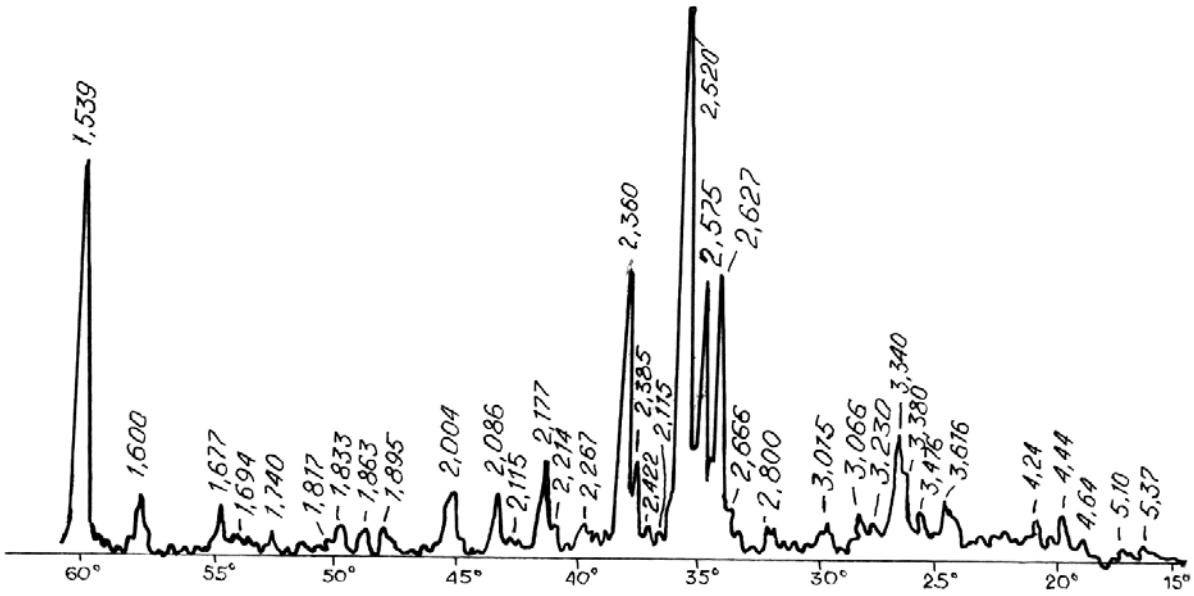

Fig. 4. SiC-1 and SiC-2 X-ray

3. CONCLUSION

On further treatment of samples received with reactive sintering on the basis of SiC and on their moulding with hot pressure method, abrupt growing of the physical-mechanical indices occur.

With hot pressure on the basis of SiC a composite with complex binder is received, which contains the same components that were formed at reactive sintering.

Introduction of Al_2O_3 Nano-powder into SiC-1 composition gives SiC-2 composite different microstructure and creation of complex binder in the phase.

SiC-2 composite has homogeneous, fine crystalline structure and higher physical-mechanical indices compared to SiC-1.

The high exploitation indices of the obtained composites determine the use of silicon carbide products in structural materials.

Acknowledgment:

We express our gratitude to Shota Rustaveli Georgian National Science Foundation. The work is done with the grant of the Foundation FR-21-1413 Grant 2022.

REFERENCES

1. M.A.Janney. Amer. Ceram. Soc. Bull., 1987, v.66, No 2. p.322-324.
2. G.C.Wei, P.F.Becher. J.Amer.Ceram.Soc. 1984. v.67, No 8, p.571-574.
3. R.Ruh, A.Zangvil, J.Barlow. Amer. Ceram. Soc. Bull. 1985. v. 64, No 10. p.1368-1373.
4. R.Ruh, L.B.Bentsen, D.P.Hasselman. J. Amer. Ceram. Soc. 1984, v.67. No 5, p. C-83-C-84.
5. R.A.Cutler, A.W.Vilkar, J.B.Holt. Ceram. Eng. Sci. Proc. 1985. v.6. No 7/8. p.15-21.
6. K.Niihara, A. Nikahira, T.Uchigava. Fract. Mech. Ceram. v.7. – Plenum Press, 1986. p.103-116.

7. Z.Kovziridze, N.Nizharadze, G.Donadze, V.Kinkladze. SiC with complex binder. Ceramics, 2(16), 2006, p.12.
8. Zviad Kovziridze, Jimsher Aneli, Natela Nijaradze, Gulnazi Tabatadze. Ceramic and Polymer Compozites. Monograph. LAMBERT Academic Publishing. Germany. 2017
9. Zviad Kovziridze, Jimsher Aneli, Natela Nijaradze, Gulnazi Tabatadze. Ceramic and Polymer Compozites. Monograph. Georgian Technical University. Tbilisi Georgia. 2016.
10. W. Kollenberg. Technische Keramik. Vulkan-Verlag Essen. Germany. 2000. S.21. 68.
11. Burggraf A. I. Korngroesse. Korngroessen-verteilung und Korngrenzen im Zusammen-schaften 27. 1977. IV. 6. s.102-114
12. Dudrova E. Kubelik I. Influence of Sintering Conditions upon the porosity and the strength of compacts. Powder Met., 3. 1979. 4. 1. P. 183-185
13. Mackenzie J. K., Schuttleworth R. Proc. Phys. Soc. London. B. 62. 1949. P.883.
14. Helda Gollisch-Szibov. Zum Zusammensetzung der Gefuegedaten und mechanischen Eigen-schaften von Porcellan. Dis zur Erlengung des grades eines Doctor Ingenieur 1979 April TU Clausthal s. 3-117.
15. Krockel 0. Der Einflus der Porositaet auf die mechanische Festigkeit von keramischen Wer-kstoffen. Silikattechnik 23.1972. 3. S. 83-87.
16. Stabenow R. Hennicke H.W. Untersuchung zum Phasenaufbau, Gufuege und mechanischen Eigenschaften von Tonerdeporcelan. Kera-mische Zeitschrift. 28. # 5. 1976 s. 227-229. # 6. 1976., s. 287-290.
17. Hestber I. Scholze H. Massenspektrometrische Untersuchungen zum Einflus der Brennatmo-sphaere auf die Blasenbildung in Porcellang-lasuren. Berichte der Deutsche Keramische Gesellschaft. 49. 1972. 1 s. 357-362.
18. Dudrova E. Kubelik I. Influence of sintering conditions upon the porosity and the strength of compacts. Powder Met. 3 1979. 4. S. 183-185.

UDC 621.9.02

THE FORMULA FOR CORRELATION BETWEEN POROUS PHASE AND MACRO-MECHANICAL CHARACTERISTICS OF THE MATERIAL

Z. Kovziridze

Georgian Technical University, Institute of Bionanoceramics and Nanocomposites Technology. 75 Kostava, 0175 Tbilisi, Georgia

E-mail: kowsiri@gtu.ge

Resume: **Goals.** Determination of the correlation of characteristics of consolidated body with content, size, distribution in matrix and shape factor of porous phase. The goal of the following paper is to determine formula for correlation between characteristics of ceramics and ceramic composite materials and porous phase, which is the weakest part of material. This will allow theorists and practitioners to correctly choose and improve technologies and technical processes.

Method. According to the study and analysis of micro- and macro structural, micro- and macro-mechanical properties of ceramics and ceramic composite materials, parameters of the formula were determined.

Results. Formula contains macro-mechanical properties, when detail is completely decomposed: mechanics on bending by three or four-point load, mechanics on shrinking, breaking, impact resistance. Morphologic characteristics: porous phase content in the matrix and its distribution, size, shape factor of pores. Correlation of given factors with others structural characteristics, such as: crystal and glass phases. Novel determination of pore distribution factor is given.

$$6\ m/p = \frac{P}{Fp \cdot Pd \cdot Pvol. \cdot Pm}$$

Where P is load, MPa; F_p - shape factor of pore; P_d – factor of distribution of pores in matrix. Value of given parameter is 1. Its evaluation is depended on researcher according to morphologic picture, size and distribution of pores in material. Factor value is varied between 1 and 0.8. if pores have equal size and are evenly distributed, factor value is 1. Factor is 0.9 if pore distribution is uneven. And 0.8 if coalescence process of pores is started. Pvol. – volume ratio of porous phase in matrix; Pm – average size of pores.

Conclusion. Created formula has collective nature and using it allows researchers and practitioners to correctly plan and precisely preform all the positions of the technological production.

Key words: Factor of distribution of porous phase in matrix, macro-mechanics, factor of pore shape, pre size, content of pores in matrix.

1. INTRODUCTION

During structural-mechanical research of ceramic materials content of porous phase, pore size, shapes and their factors[1], are they closed, piercing or half-piercing, their distribution in matrix play important role (fig. 1). It's obvious, that pore is weakest part of material regardless it's open or closed. We review closed porous phase, when material is anointed, consolidated and shows its best properties. Porous phase drastically lowers mechanical properties of material, especially in cases, where its content is high, exceeds 8-9% due to different technological reasons according to Budworth parameters [1] and have larger size then 5-7 μm.

Low pore content in matrix, less than 1-3%, their small size, between 0.1 and 5 micron, even distribution and spherical shape guarantees not only high mechanical properties, but excellent exploitation properties, such as: thermal hardness, thermal resistance, exploitation duration, resistance against thermal and air thermal attacks [2], electrical properties in microcircuits, wear resistance during cutting, under conditions of mechanical blow, difficult operating loads and stresses like electricity transfer lines [3-5] etc. Therefore, it's important to determine correlation formula between macro-mechanical properties of material and porous phase.

When open porosity according to water absorption is zero or close to it, less than 0.5%, closed pore content in matrix ranges between 0.1-9% volume percent. [1]. Fig. 1 shows pore types [6].

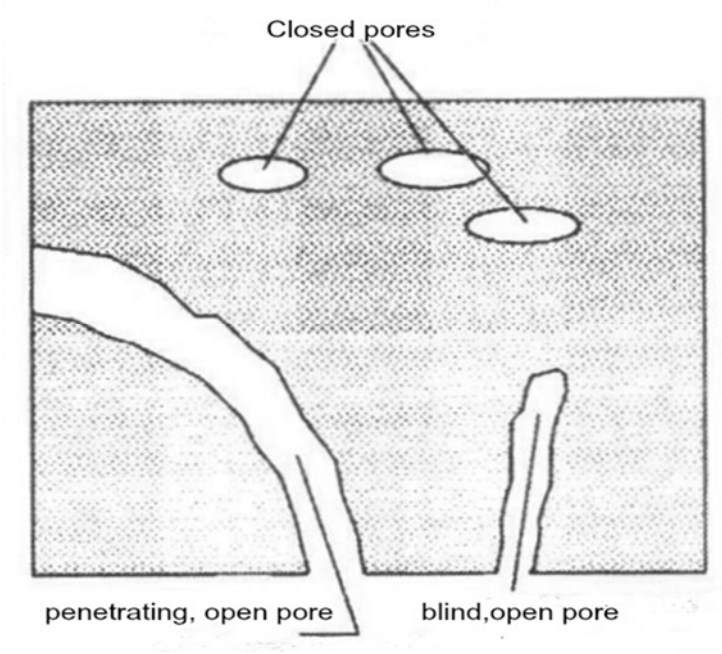

Fig. 1. Schematic representation of pores

[1] The shape factor means the ratio of the largest characteristic size to the smallest, which allows us to characterize the given phase, its units and the set of pores in a particular case.

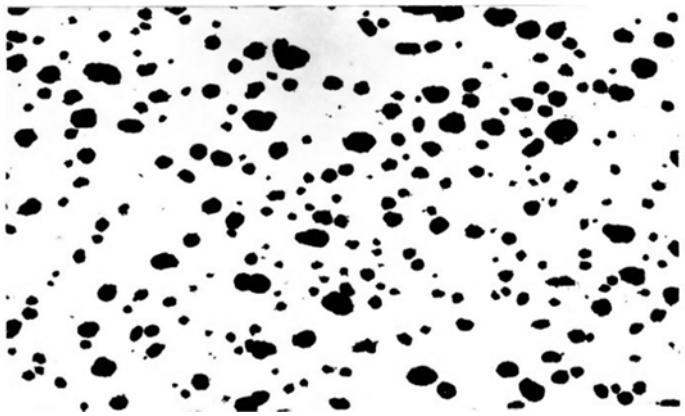

a)

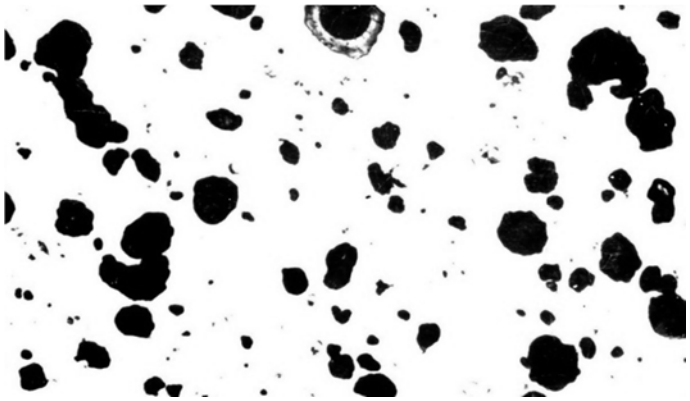

b)

Fig. 2. Morphological picture of the closed porous phase of celsian electro-ceramics.
a) at the lower limit of the temperature range of the sintering at 1410^{0}C
b) at the upper limit of the temperature interval of the sintering at 1500^{0}C.
The coalescence [2] process of pores is in progress

2. MAIN PART

Fig. 2 shows three component system BaO-Al_2O_3-SiO_2 samples fired in the sintering temperature range of Celsian ceramics. In both cases, the open porosity is equal to zero according to water absorption. 1470^{0}C is the optimal tempering temperature of this ceramic, that is, when the material is ready for industrial use.

At 1500^{0}C, the ceramic is at the upper limit of the sintering interval, the water absorption is zero, but the pores coalesce in the matrix, which can be clearly seen in Figure b). It is obvious that in this case the mechanical strength decreases and is 66 MPa for the given material.

[2] Coalescence, the growth of pores in a solid body, accompanied by a decrease in their total surface area while the total volume remains unchanged. The process of pore coalescence is observed in the last stages of the coating and is determined by the increase in the size of the large pores, as a result of the vacancy solubility of the small pores.

At 1410⁰C, the mechanical bending strength is 79 MPA. In this case, the pore redistribution factor is taken as 0.8. 79x0.8=63.2. The difference between 66 and 63.2 is an error of -4.24 %. In many other cases, the calculated pore distribution factor in the material is within this error [7-8]. The remaining parameters of the formula are calculated from optical and electron-microscopic images obtained as a result of structural research.

Fig. 3 a) and b) show the results of linear closed porosity analysis for the same composition of electrotechnical ceramics baked at temperatures of 1410⁰C and 1500⁰C (Fig. 2).

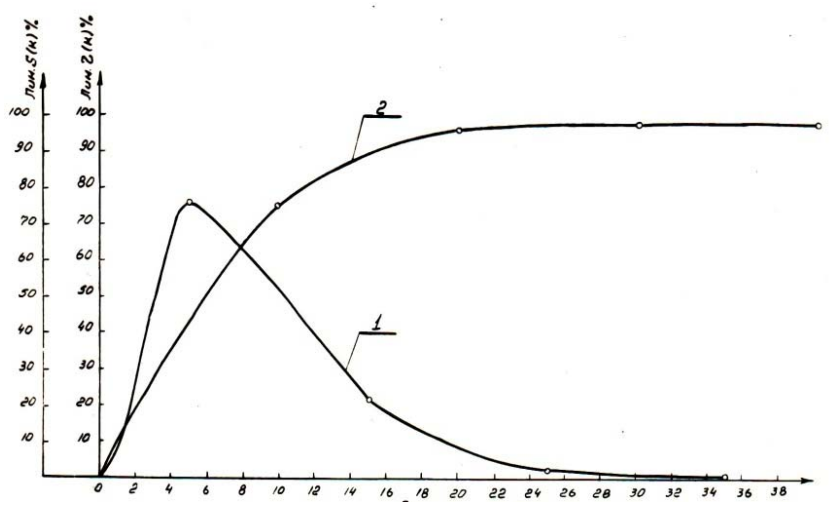

a

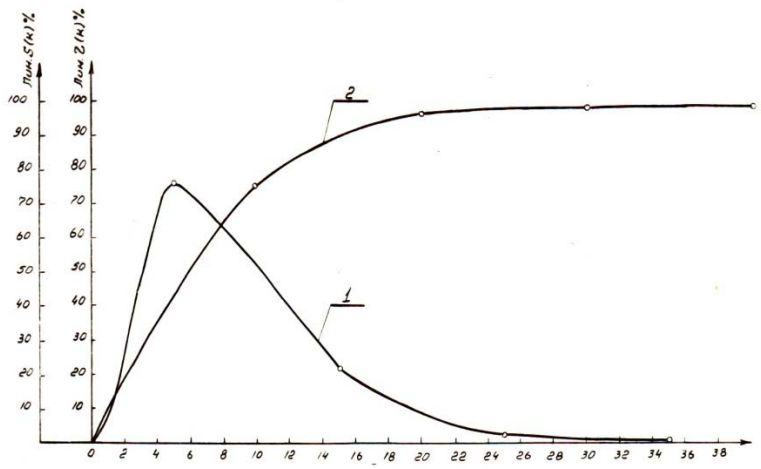

b

Fig. 3 Linear analysis of closed porosity of electroceramic material.
a) Baked at 1410⁰C, b) Baked at 1500⁰C. 1. Frequency of pores.
2. Total frequency of porosity.

Fig. 3 shows the process of formation of closed pores and their distribution in the matrix at the initial and final stages of material sintering. At the initial stage of sintering at 1410^{0}C (Fig. 3 a), the pore distribution curve 1 shows that the material contains 75% of the total porosity with pores less than 5 μm in size, while the total curve (curve 2) shows 95% of the total porosity with pores with a size of less than 14 μm. At the final sintering stage at 1500^{0}C, the material contains 70% of pores less than 4 μm in size (curve 1) and 90% of pores less than 12 μm in size. Only 5% and 10% of the pores at the initial and final stages of sintering, respectively, have sizes larger than the optimum, which is generally accepted for ceramic materials, i.e. 5 μm. The average size of said pores is more than 9 μm. McKenzie and Shutlerworth derived an equation for the rate of material settling during heat treatment [9]. The effect of surface tension is equal to the pressure -2y/r that exists inside every pore, and if the material is incompressible it is equal to the hydrostatic pressure +2y/r exerted on the mass

$$\frac{d\rho}{dt} = \frac{2}{3}\left(\frac{4\pi}{3}\right)^{1/3} n^{1/2} \frac{y}{n}(1-\rho)^{2/3} \rho^{1/3}$$

Where p - is the relative density (the ratio of the bulk weight to the specific weight), n - the number of pores in the unit volume of the real material. The task is to establish a connection between the properties of a porous viscous material and the properties of a dense material. The number of pores depends on their size and relative density

$$n\frac{4\pi}{3} r3 = \frac{\text{Pore volume}}{\text{solid material velocity}} \quad \frac{1-\rho}{\rho}$$

$$n^{1/3} = \left(\frac{1-\rho}{\rho}\right)^{1/3} \left(\frac{3}{4\pi}\right)^{1/3} \frac{1}{y}$$

Combining the equations gives

$$\frac{d\rho}{dt} = \frac{3\gamma}{2\, r0n}(1-\rho)$$

where r_o - is starting radius of particles

Upon reaching a relative density of 0.6, spherical pores are rapidly formed. For the case of complete hardening, we will get

$$t_{sek} = \frac{1,5 r_0 \eta}{y}$$

The above relationships can be successfully used to describe the process involving the thyroid phase. Helga Golish-Scibov [10] investigated the effect of porosity on the mechanical strength of porcelain and took the average optimal pore size of 5 μm, finding that the strength of the material depends not only on porosity, but also on their size and shape. For comparative analysis, morphological of pores in hard porcelain is presented in Fig. 4.

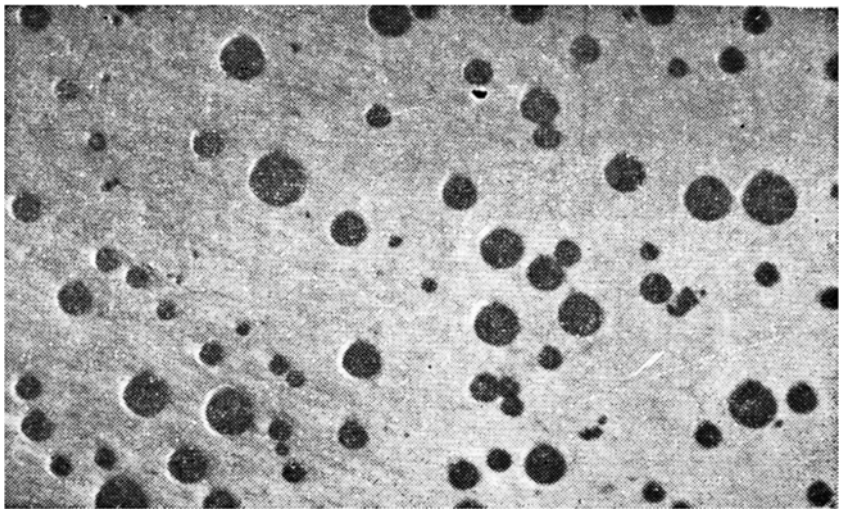

Fig. 4 pore structure in hard porcelain, baked at 1420^{0}C . X95

From Figure 4, it is clear that the material is well sintered, i.e. consolidated, and it can be used for industrial use. It should be noted, that obtaining a perfectly consolidated material is a difficult technological process and is rare. From the morphological picture, it can be seen that the pores are round in shape, but uneven in size and the difference in diameter is quite large. It seems that at some technological position out of the 26 operations required to obtain such material, a technological breach occurred, from which no technology is immune. It probably refers to the process of forming and heat treatment. In this case, the distribution factor in the pore matrix will be estimated as 0.9. The uniformly round shape of the pores throughout the matrix ensures high mechanical properties of porcelain. The unbaked product consists of individual grains separated by pores. Depending on the type of raw materials and production methodology, the number of pores is 25-60% by volume. To improve the technical properties of materials, it is necessary to significantly reduce the content of pores in the matrix. Budworth [1] investigated synthesis theory in relation to porosity and mathematically calculated the effect of surface energy on a cylindrical pore system. He showed that the total porosity in each synthesized mass is about 9%. The effect of porosity on mechanical properties is described in work [11]. Stabenov and Henicke investigated the structure and mechanical properties of porcelain containing aluminum oxide as a function of firing temperature and dwell time at the final temperature. They found a constant and continuous change in the distribution of pores in the structure and the dependence of strength and elasticity on porosity [12].

The size and distribution of pores in the matrix changes systematically. During baking, the atmosphere in the oven affects the content of pore gases through changes in the partial pressure of water vapor [13-14]. The effect of particle shape

and production technology on the formation of pores during the synthesis process is given in the work [8]. Oel [15] investigated the synthesis process depending on the pore structure and showed that a slight change in the pore radius causes a drop in the synthesis process, and when the maximum synthesis temperature is reached, the structure partially swells. which is confirmed in the case of our material at 1500^{0}C (Fig. 2 b). The pores in the material can change shape and become elongated pores. However, it is not necessary to change their overall size. Both the shape and the size of the pore change mainly during the thermal treatment process. This process is confirmed by the ceramics presented by us at 1500^{0}C. Table 1 shows the dynamics of porosity change depending on temperature. Analysis was performed on a Zeis-Wang instrument at the Clausthal Technical University, Germany.

Table 1

Matrix Properties of Celsian Electroceramics

Temperature ^{0}C, > indicator∨	1380	1410	1440	1470	1500	1550
Average pore size, d-μm	7.6	8.0	7.8	5.1	12.8	26.4
The average distance between the pores in the matrix is l-μm	43.6	48.5	92.2	80.0	98.0	380.0
Pore content, V %	16.0	14.0	8.8	8.3	9.8	12.8

Table 1 shows the data of the porous structure of the electroceramic celsian material presented by us. The table clearly shows the dynamics of changes in pore sizes depending on temperature. 1470^{0}C is the baking temperature when the material contains pores with the minimum size of 5.1 μm, therefore the distance between the pores in the matrix is optimal - 80 μm and the percentage of pores is minimum - 8.3 %. It is this temperature that can be considered the temperature of use of this composition in the Celsian electroceramic industry. Let's enter this data into the mathematical formula we have presented. we get:

$$\text{Б m/p} = \frac{P}{Fp \cdot Pd \cdot Pvol. \cdot Pm} = \frac{79}{1.5x0.9x8.3x5.1} = 57.15 \text{ MPa}$$

Thus, for this particular material, the dependence of the macro-mechanical characteristic on the porous phase is 57.15 MPa.

3. CONCLUSION

in the formula given by us, which shows how much the macro-mechanical characteristics of materials, i.e., their complete disintegration, depends on the size, shape, distribution and content of pores in the matrix, on the pore shape factor, the influence of the weakest phase of the structural components of the consolidated material on the set of properties is taken into account, Significantly determine the ability and duration of work in the goods industry.

In the process of thermal processing, the most important thing is the dynamics of the formation of pores, their distribution in the matrix, the formation of the shape, which is shown in our research, taking into account the physico-chemical processes that take place during thermal aggression.

The important factor here is the redistribution of pores in the matrix, which is a novelty. Our formula provides a complete answer to the correlation between the morphology of the porous phase and the macromechanical properties of ceramics and can be used for all types of ceramics and ceramic composites that work in advanced technologies, in many fields of technology, in domestic conditions.

ACKNOWLEDGMENT:

We express our gratitude to Shota Rustaveli Georgian National Science Foundation. The work is done with the grant of the Foundation FR-21-1413 Grant 2022.

REFERENCES

1. Budworth D.W. - Theory of pore closure during sintering. Trans. Brit. Ceram. Soc. 69. 1970 p.29-31
2. Zviad Kovziridze, Hans Walter Hennicke, Fridrich Kharitonov. - Thermomechanics of Ceramics. Monograph. Fachhochschule Karlsruhe Hochschule fuer Technik. Karlsruhe. Germany. 1998
3. Zviad Kovziridze, Hans Walter Hennicke, Fridrich Kharitonov - Barium-containing electro ceramics against thermal shocks Monograph. Tbilisi State University. Tbilisi. Georgia. 1992
4. Zviad Kovziridze, Jimsher Aneli, Natela Nijaradze, Gulnazi Tabatadze. - Ceramic and Polymer Compozites. Monograph. LAMBERT Academic Publishing. Germany. 2017

5 Zviad Kovziridze, Jimsher Aneli, Natela Nijaradze, Gulnazi Tabatadze. - Ceramic and Polymer Compozites. Monograph. Georgian Technical University. Tbilisi Georgia. 2016.

6. W. Kollenberg. - Technische Keramik. Vulkan-Verlag Essen. Germany. 2000. S.21. 68.
7. Burggraf A. I. - Korngroessenverteilung und Korngrenzen im Zusammenschaften 27. 1977. IV. 6. s.102-114.

8. Dudrova E. Kubelik I. - Influence of Sintering Conditions upon the porosity and the strength of compacts. Powder Met., 3. 1979. 4. 1. P. 183-185
9. Mackenzie J. K., Schuttleworth R. - Proc. Phys. Soc. London. B. 62. 1949. P.883.
10. Helda Gollisch-Szibov. - Zum Zusammensetzung der Gefuegedaten und mechanischen Eigenschaften von Porcellan. Dis zur Erlengung des grades eines Doctor Ingenieur 1979 April TU Clausthal s. 3-117.
11. Krockel 0. - Der Einflus der Porositaet auf die mechanische Festigkeit von keramischen Werkstoffen. Silikattechnik 23.1972. 3. S. 83-87.
12. Stabenow R. Hennicke H.W. - Untersuchung zum Phasenaufbau, Gufuege und mechanischen Eigenschaften von Tonerdeporcelan. Keramische Zeitschrift. 28. # 5. 1976 s. 227-229. # 6. 1976., s. 287-290.
13. Scholze H. Kausku W. - Blasverteilung in Porcelanglasuren. Keramische Zeitschrift. 20. # 12. 1968. S. 277-278.
14 Hestber I. Scholze H. - Massenspektrometrische Untersuchungen zum Einflus der Brennatmosphaere auf die Blasenbildung in Porcellanglasuren. Berichte der Deutsche Keramische Gesellschaft. 49. 1972. 1 s. 357-362.
15. Oel H.J. - Das Sintern von Glasern als Auswirkung von Zaehigkeit und Oberflaechenspannung. Berichte DKG. 37. 1960. 9. S. 424-428.

UDC 541.11

METHOD OF CALCULATION OF INITIAL PARAMETERS FOR THERMODYNAMIC EVALUATION OF OBTAINING VARIOUS USING CHIATURA MANGANUM ORE ENRICHMENT WASTE

N. Rachvelishvili, V. Gordeladze, T. Tsilosani

Georgian Technical University. Faculty of Chemical Technology and Metallurgy. Department of Chemical and Biological Technologies, Department of metallurgy, metals science and metal processing. Georgia, 0175, Tbilisi, Kostava str.69

E-mail: nana_rachvelishvili@mail.ru

Resume: **Purpose.** The aim of the work is to calculate the thermodynamic initial parameters for obtaining new solid materials using raw materials by using a modified method of the additive rule.

Method for protection: For the correct choice of ingredients to be summarized for each substance, by using "structural ingredient system additivity method", which allowed them to determine the standard molar values of thermodynamic.

Results: The values of enthalpy of formation $\Delta H_{f,298}$ and Gibbs free energy ΔG^0_{f298} determined by this method give an error that does not exceed 2% and the error of entropy $\Delta S^0_{f,298}$ and heat capacity $C_{p,298}$ 3-4%, which is acceptable for thermodynamic assessment of any reaction.

Conclusion: The proposed method was tested with the participation of many complex minerals contained in Chiatura Manganes ore enrichment waste. Comparing the theoretical results obtained to assess their interaction with each other and with the components gave us a coincidence with experimental one.

Key words: thermodynamic parameters, additivity method, technogenic raw material, enthalpy, Gibbs free energy.

1. INTRODUCTION

In technologies for obtaining new solid materials, technological raw materials are more widely used. Technogenic raw material is a multimineral system in which the number of components reaches 30. In the role of man-made materials, Chiatura manganese ore enrichments waste was used.

In the work, it is proposed to calculate the thermodynamic initial parameters for obtaining new solid materials using raw materials using a modified method of the additive rule. The method allows calculation of initial thermodynamic parameters: ΔH^0_{f298}, ΔG^0_{f298} and ΔS^0_{f298}, $C_{p,\ 298}$ 98% accuracy. The calculation is based on the Jibs Free Energy minimization method derived from all three laws of chemical thermodynamics. For the realization of the method, the Ulich first and second approximation, the Schwarzman-Temkin approach and the classical method are used.

Detailed analysis of information sources showed that among the components there are minerals of such simple and complex composition, the standard molar values of the abovementioned parameters are unknown. In addition, for most complex minerals (compounds), these parameters are known, although the quantities cited in various sources are distinguished by unevenness not allowed for thermodynamic analysis.

All this often makes it practically impossible to predict and determine the interaction of the components contained in the prepared of one or another material of waste of various enterprises and other man-made raw materials. Many methods have been proposed [1-4] to determine the status of the ΔH^0_{f298}, ΔG^0_{f298} and ΔS^0_{f298} but their use for multimineral systems is associated with many problems, since date extraction is often practically impossible.

For the correct choice of ingredients to be summarized for each substance, we used "structural ingredients system additivity method", which allowed them to determine the standard molar values of thermodynamic parameters for thermodynamically unknown silicates in a separate crystallochemical group of silicate classification.

2. MAIN PART

Below is an attempt to use this method in relation to borates. To realize the derived Jibs free Energy minimization, the Ulich I and II approximation, the Shwartzman-Temkin approach and the classical method are used [5-8].

Calculation of the reaction ΔG_{298} and the equilibrium constant

$$Na_2O \cdot B_2O_3 + CaCO_3 \rightarrow$$

$$\rightarrow Na_2O \cdot B_2O_3 + CaO \cdot B_2O_3 + CO_2$$

The reaction is known from the initial thermodynamic date that are given in Table 1.

Table 1

Substance	ΔH^0_{298} kkal/mol	ΔS^0_{298} kal/mol K	a	$b \cdot 10^3$	$c \cdot 10^{-5}$	ΔG^0_{298}
$Na_2O \cdot 2B_2O_3$	-786590	45,3	48,81	18,96	-8,17	-800089,4
$CaCO_3$	-288450	22,2	24,98	5,24	-6,2	-295065,6
$Na_2O \cdot B_20_3$	-467020	35,14	45,57	3,24	-17,88	-477491.72
$CaO \cdot B_2Q_3$	-485410	25,06	31,02	9,76	-8,07	-492877,88
CO_2	-94052	51,06	10,55	2,16	-2,04	-109267,88
	28558	43,76	13,35	-9,04	-13,6	15517,52

Calculation the Ulich first approximation, we get:

Table 2

T	ΔH^0_{298}	ΔS^0_{298}	ΔG_{298}	LgK
298	28558	43,76	15517,52	-11,378924
400	28558	43,76	11054	-6,03852
600	28558	43,76	2302	-0,8383495
800	28558	43,76	-6450	1,76173575
1000	28558	43,76	-6450	3,3217869
1200	28558	43,76	-23954	4,361821
1300	28558	43,76	-28220	4,76183412
1500	28558	43,76	-37082	5,4018551

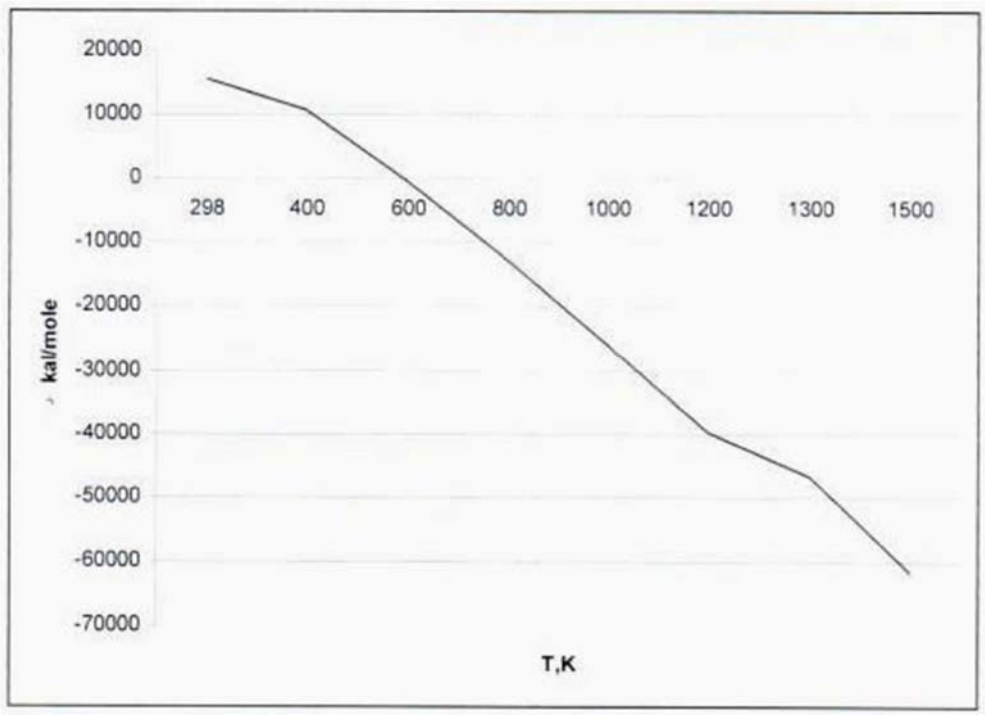

Fig.1. Graph of Energy and Temperature dependence

Table 3

From the second Ulich calculation, we get:

T	ΔH^0_{298}	ΔS^0_{298}	ΔG_{298}	LgK
298	28558	43,76	15517,52	-11,3789239
400	28558	43,76	10844,672	-5,924169417
600	28558	43,76	730,438	-0,266013176
800	28558	43,76	-10291,596	2,811013176
1000	28558	43,76	-21994,48	4,806010759
1200	28558	43,76	-34222,82	6,231686356
1300	28558	43,76	-40511,4745	6,809351266
1500	28558	43,76	-53384,3525	7,776671615

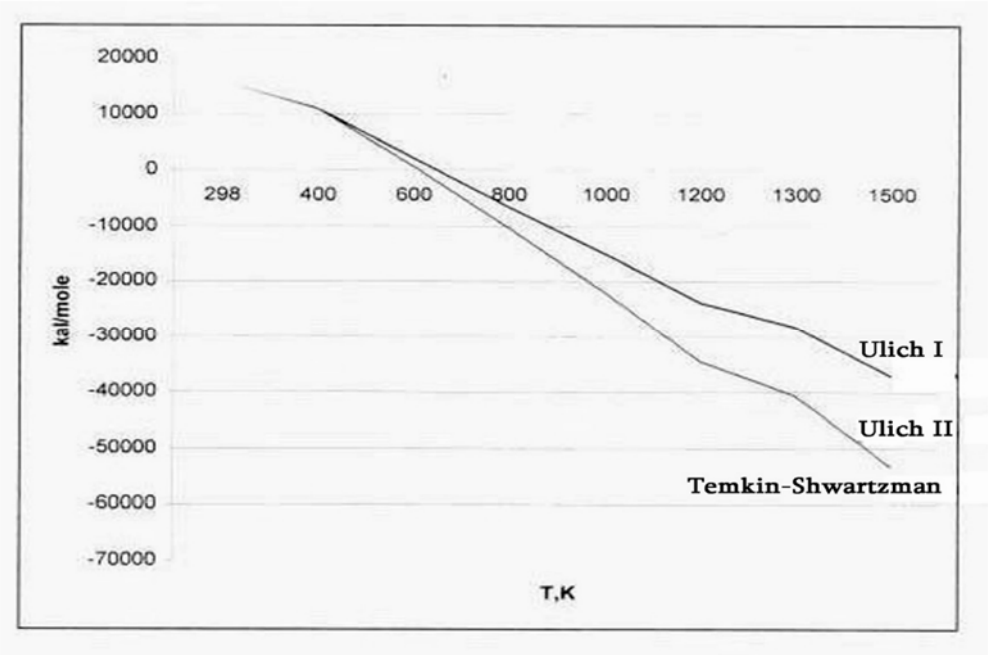

Fig. 2. Relative graph Ulich I, Ulich II and Temkin-Shwartzman dependence on Energy

Table 5

By the Temkin-Shwartzman method

T	ΔH^0_{298}	ΔS^0_{298}	ΔG_{298p}	lgK
298	28558	43,76	15517,52	-11,3782924
400	28558	43,76	10605,7072	-5,793629
600	28558	43,76	-473,60576	0,172479214
800	28558	43,76	-12816,7125	3,500722572
1000	28558	43,76	-26007,5812	5,682912843
1200	28558	43,76	-39781,3131	7,243840987
1300	28558	43,76	-46878,9057	7,879617807
1500	28558	43,76	-61412,3609	8,946137613

Table 4

With classic method

T	ΔH^0_{298}	ΔS^0_{298}	ΔG_{298p}	lgK
298	28555,9975	43,76086051	15517,2636	-11,3781044
400	29917,6975	44,37059868	10809,7605	-5,9059817
600	32587,6975	47,59977454	-1,86472323	0,000679101
800	35257,6975	50,79352604	-12076,8208	3,298630545
1000	37927,6975	53,570022996	-25012,2299	5,46541888
1200	40597,6975	55,9769394	-38614,3273	7,031342726
1300	41932,69750*	57,06595146	-456277,7369	7,669315715
1500	44602.6975	59,05685581	-60027,2837	8,744368931

Table 6

Relative error betwine methods

T	Ulich I	Ulich II	Temkin-Shwart.	Classic	Ulich I-Classic	Ulich II - Classic	T.– Shwart. Classic
248	15517,52	15517,52	15517,52	15517,26	1,65253E -5	1,65253E-05	1,6525E-05
400	11054	10844,67	10605,71	10809,76	0,022095121	0,0032119228	0,019239955
600	2302	2302	730,438	-473,606	1,000810045	1,00025522884	0,99606271
800	-6450	-10291,6	-12816,7	-12076,8	0,872375323	0,137204878	0,038271581
1000	-15202	-21994,5	-26007,6	-25012,2	0,645324954	0,137204878	0,038271581
1200	-23954	-34222,8	-39781,3	-38614,3	0,612020008	0,128321023	0,029335026
1300	-37082	-40511,5	-46878,9	-45627,7	0,610580194	0,126291686	0,026689377
1500	-37082	-53384,4	-61412,4	-60027,3	0,618771472	0,124435924	0,02255372

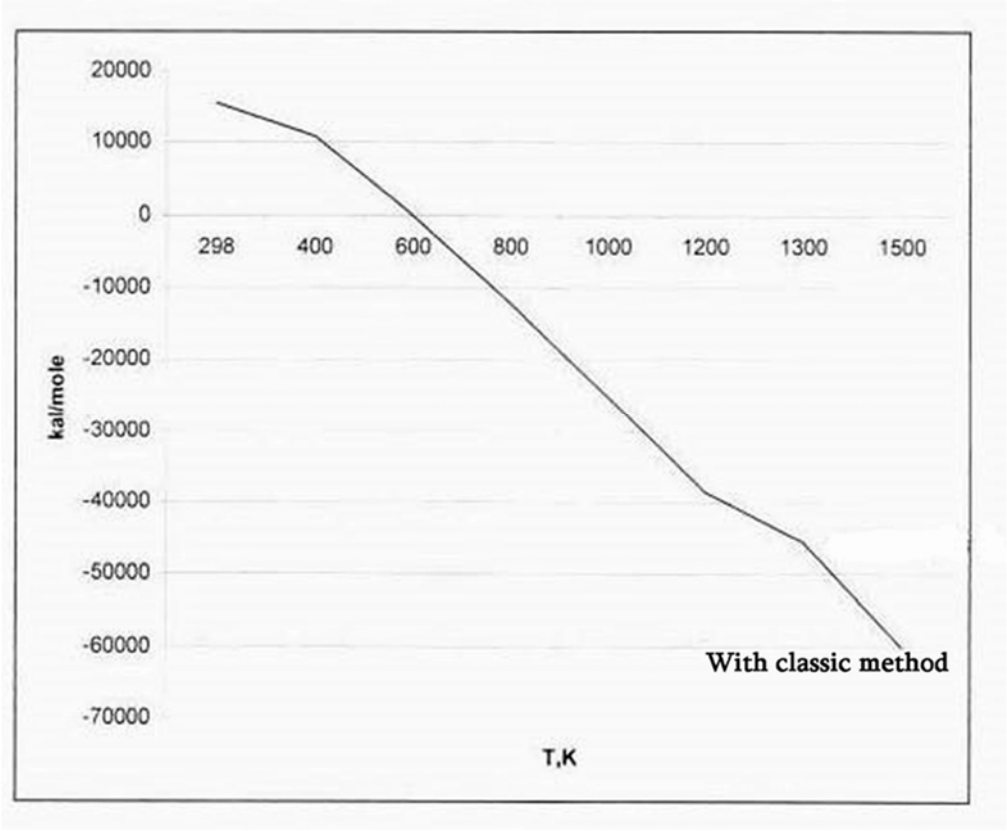

Fig. 3. Classic Method

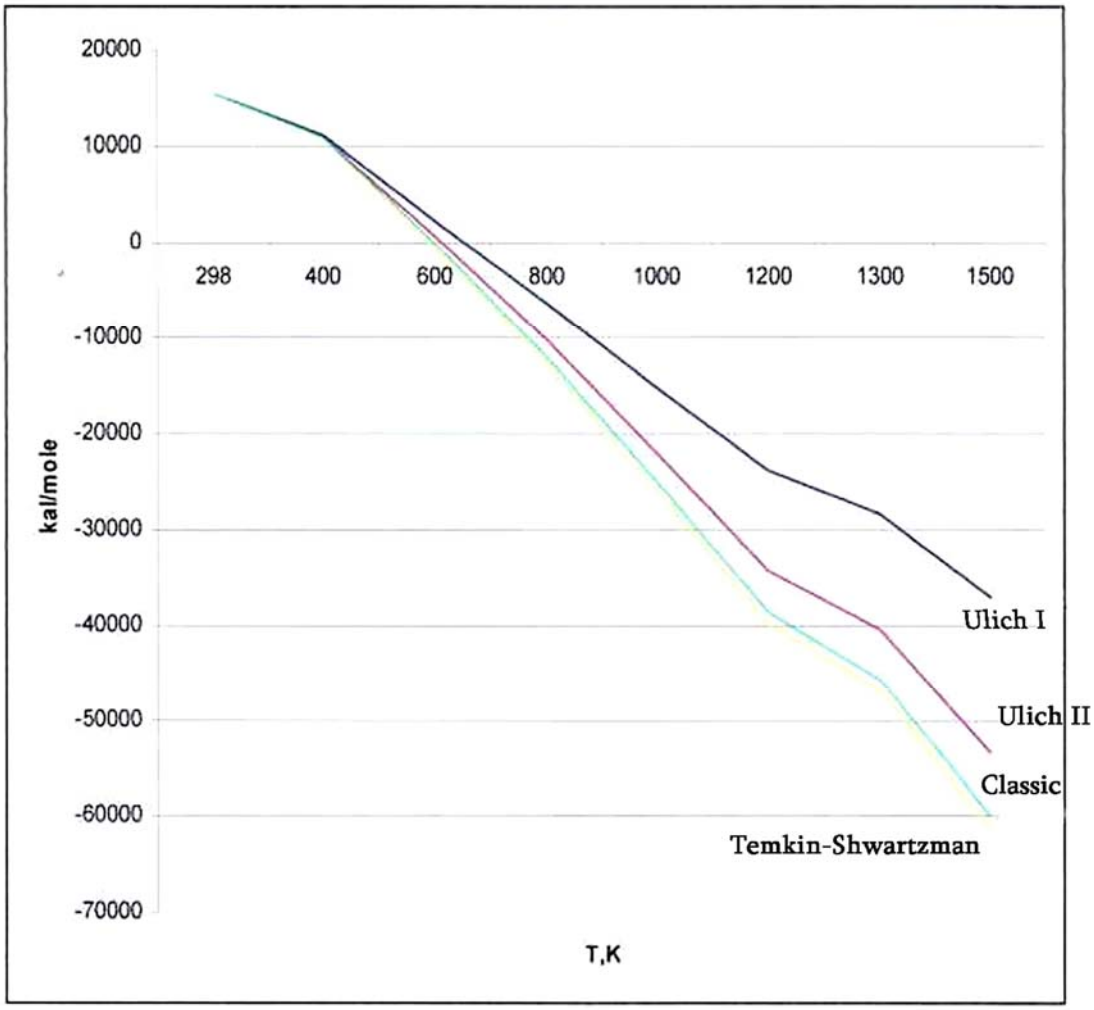

Fig. 4

To use this method it is necessary to get acquainted with the issues of crystallochemical classification of borates.

The borat formation can be derived by the equation:

$$2(H_3BO_3) + Na[B(OH)_4] + Na[B(OH)_4] \cdot 2H_2O + H_2O \rightarrow$$
$$\rightarrow Na_2[B_4O_5(OH)_4] \cdot 8\ H_2O$$

The tinkantolic formation can be derived by the equation:

$$2(H_3BO_3) + Na[B(OH)_4] + Na[B(OH)_4] \cdot 2H_2O + H_2O \rightarrow$$
$$\rightarrow Na_2[B_4O_5(OH)_4] \cdot 8\ H_2O$$

The kenrity:

$$2Na[B(OH)_4] + B_2O_3 \rightarrow Na_2[B_4(OH)_2] \cdot 3\ H_2O$$

It follows that:

$$\Delta H^{\circ}_{f,298,Bor} = \Delta H^{\circ}_{f,298,Na\,BO2\cdot 2H_2O} + \Delta H^{\circ}_{f,298,B_2O_3\cdot 3H_2O} + \Delta H^{\circ}_{f,298,NaBO_2.4H20} + \Delta H^{\circ}_{f,298,H20}$$
$$= 523{,}10 - 378{,}11 - 520{,}11 - 57{,}796 = -1479{,}09 kcal/Mol$$

$$\Delta H^{\circ}_{f,298,Tin} = \Delta H^{\circ}_{f,298,Na_2O\cdot 2H_2O} + \Delta H^{\circ}_{f,298,B_2O_3\cdot 3H_2O} + \Delta H^{\circ}_{f,298,NaBO_2} =$$
$$= -378{,}11 - 523{,}10 - 233{,}51 = -1134{,}72 kcal/Mol$$

$$\Delta H^{\circ}_{f,298,ker} = 2\Delta H^{\circ}_{f,298,NaBO_2\cdot 2H_2O} + \Delta H^{\circ}_{f,298,B_2O_3} =$$
$$= 756{,}22 - 304{,}20 = = 1060{,}42 kcal/Mol$$

It is necessary to compare the obtained quantities with the date available in information sources. Fully thermodynamic parameter date is known only for borat ($\Delta H_{f,\ 298,\ BOr}$ = 1503,1 kcal/mol) and tinkalton ($\Delta H_{f,298,\ Tin}$ =-1145,3 kcal/mol). However unspecified for kernite ($\Delta H_{f,\ 298,\ Ker}$ = -1081,7kcal/mol). In this case the rectifier and leveling coefficients will be equal:

$$K_{c.Bor} + K_{\ c.Tin} + K = \frac{-1503{,}1}{-1479{,}09} + \frac{-1145{,}3}{-1134{,}72} + \frac{-1081{,}7}{-1060{,}42} =$$
$$= 1{,}0129 + 1{,}0093 + 1{,}02 = 3{,}0419$$

$$K_{subst.} = \frac{\sum K_{\vartheta}}{3} = \frac{3{,}0419}{3} = 1{,}01397 \approx 1{,}014$$

The get the true values, $\Delta H_{f,\ 298}$ obtained by calculation should be multiplied by $K_{subst.}$ The obtained results are given in the table [9-11]. The values of enthalpy of formation $\Delta H_{f,\ 298}$ and Gibbs free energy ΔG^0_{f298} determined by this method give an error that does not exceed 2% and the error of entropy $\Delta S^0_{f,\ 298}$ and heat capacity $C_{p,298}$ 3-4%, which is acceptable for thermodynamic assessment of any reaction.

Method of structural ingredients additivity is the result of information analysis available in some areas of theory and practice of solid crystal bodies.

The proposed method was tested with the participation of many complex minerals contained in Chiatura Manganes ore enrichment waste. Comparing the theoretical results obtained to assess their interaction with each other and with the components gave us a coincidence with experimental one.

Table 7

The course and results of the borates $\Delta H_{f,298}$ report

Borat	Borat $\Delta H_{f,298}$ kcal/mol	Structural Ingredients and their $\Delta H_{f,298}$		Received by account $\Delta H_{f,298} = -q$, Kcal/mol	Correction factor (Kc) $K_c = \frac{\Delta H_{f,298}}{q}$	Leveling coefficient ($K_{subst.}$) $K_{subst} = \frac{\sum K_{g,o}}{n}$	Result $q \cdot K_{subst} - \Delta H_{f,298}$ Kcal/mol	Error		Note
		Struct. Ingred.	$\Delta H_{f,298}$ Kcal/mol					$\Delta H_{f,298} - -\Delta H_{f,29}$ Kcal/mol	%	
1	2	3	4	5	6	7	8	9	10	11
Borat-Tincaltonite group (class B)										
$Na_2[B_4O_5(OH)_4] \cdot 8H_2O$ $Na_2O \cdot 2B_2O_3 \cdot 10H_2O$ (Bor)	-1503,1	$2(H_3BO_3)$ Na[B(OH)4]· Na[B(OH)4]2H2O H2O	-523,10 -378,11 -526,11 -57,796	-1479,09	1,0129	1,0141	-1499,945	-3,159	0,21	For minerals of this group, only Borat is distinguished. $\Delta H_{f,298}$ magnitude is characterized by a high degree of reliablity and a very insignificant difference. These magnitudes are reported in news sources.
$Na_2[B_4O_5(OH)_4] \cdot 3H_2O$ $Na_2O \cdot 2B_2O_3 \cdot 5H_2O$ (Tin)	-1145,3	Na[B(OH)4] $NaBO_2$ $2(H_3BO_3)$	-378,11 -233,51 -523,10	-1134,72	1,0093		-1150,720	+5,420	0,47	
$Na_2[B_4O_5(OH)_4] \cdot 3H_2O$ $Na_2O \cdot 2B_2O_3 \cdot 4H_2O$ (Ker)	-1081,7	$2Na$[B(OH)4] B_2O_3	-756,22 -304,20	1060,42	1,0201		-1075,37	-6,330	0,59	
Cotoite group (class A)										
$Ca_3[BO_3]_2$ $3CaO \cdot B_2O_3$ Calcium Borate	-819,57	$2CaO \cdot B_2O_3$ CaO	-653,54 -151,82	805,36	1,0176	1,0176	-819,53	-0,04		For this group of Borates, there is only one benchmark – calcum orthoborate. Therefore the $\Delta H_{f,298}$ utility prescribed for other minerals is possible.

3. CONCLUSION

Technological raw materials are more widely used. Technogenic raw material is a multimineral system in which the number of components reaches 30. In the work, it is proposed to calculate the thermodynamic initial parameters for obtaining new solid materials using raw materials using a modified method of the additive rule. The method allows calculation of initial thermodynamic parameters: ΔH^0_{f298}, ΔG^0_{f298} and ΔS^0_{f298}, $C_{p,\ 298}$ 98% accuracy.

REFERENCES

1. В.А. Киреев. Методы практических расчетов в термодинамике химических реакций. М., Химия, 1975 – 536с.
2. Г.Г. Гвелесиани, Д.И. Багдавадзе. Расчетные методы определения термодинамических функций неорганических веществ и их применение при полном термодинамическом анализе металлургических процессов. Тб., Универс, 2006 – с. 5-74.
3. А.Н. Винчелл, Г.В. Винчелл. Оптические свойства искуственных минералов. М., Мир, 1967 – 528 с.
4. В.И. Бабушкин, Г.М. Матвеев, О.П. Мчедлов -Петросян. Термодинамика силикатов. М., Стройиздат, 1986 – 408 с.
5. Salema P.P. Физическая Химияю Термодинпмика. М: Физматлит, 2004. -352с.
6. Киреев В.А. Методы практических расчетов в термодинамике химических реакций. М: Химия, 1975. -536с.
7. Цагареишвили Д.Ш. Сб. Термодинамические исследования неорганических материалов Тб., Мецниереба, 1980, с. 42-62.
8. Ландия Н.А. Расчет высокотемпературных теплоемкостей твердых 27 неоргонических веществ по стандартной энтропи. Тбилиси. В. Кн. Избранные труды. Тбилиси: Мецниереба, 1990, с.10-196.
9. Гвелесиани Г.Г., Багдавадзе Д.И. Расчетные методы определения термодинамических функций неоргонических веществ и их применение при полном термодинамическом анализе металлических процессовю Тбилиси, ,,Универсал,, 2006.
10. Краткий справочник физико-химических величин. ПА/р А.А. Равеля и А.М. Пономаревой. Л: Химия, 1983. – 92с.
11. Саруханашвили А.В., Мшвилдадзе М., Капанадзе М. Физическая химия для начинающих (на гр. Яз), Тбилиси, ТУ, 2008. – 230 с.

THE GEORGIAN CERAMISTS ASSOCIATION JOINED
THE INTERATIONAL CERAMIC FEDERATION SINCE 2008

THE GEORGIAN CERAMISTS ASSOCIATION HAS BEEN A MEMBER
OF THE EUROPEAN CERAMIC SOCIETY SINCE 2002

THE GEORGIAN CERAMIC ASSOCIATION WAS FOUNDED IN 1998
THE MAGAZINE WAS FOUNDED IN 1998

TBILISI, "CERAMICS AND ADVANCED TECHNOLOGIES", Vol. 25. 1(49). 2023

Reference of magazine is obligatory on reprinting

Print circulation 3. Contract amount 50. Printed A4 format.

GEORGIAN CERAMISTS ASSOCIATION. Tbilisi. Str. Kostava 69. Phone: +995 599 151957
E-mail: kowsiri@gtu.ge, Zviad Kovziridze

http://www.ceramics.gtu.ge